UCRL-19133

c.3

VAPORIZATION MECHANISM OF ICE SINGLE CRYSTALS

John Gordon Davy
(Ph. D. Thesis)

December 1969

AEC Contract No. W-7405-eng-48

RECEIVED
LAWRENCE
RADIATION LABORATORY

MAY 20 1970

LIBRARY AND
DOCUMENTS SECTION

TWO-WEEK LOAN COPY

This is a Library Circulating Copy which may be borrowed for two weeks. For a personal retention copy, call Tech. Info. Division, Ext. 5545

UCRL-19133 c.2

LAWRENCE RADIATION LABORATORY
UNIVERSITY of CALIFORNIA BERKELEY

DISCLAIMER

This document was prepared as an account of work sponsored by the United States Government. While this document is believed to contain correct information, neither the United States Government nor any agency thereof, nor the Regents of the University of California, nor any of their employees, makes any warranty, express or implied, or assumes any legal responsibility for the accuracy, completeness, or usefulness of any information, apparatus, product, or process disclosed, or represents that its use would not infringe privately owned rights. Reference herein to any specific commercial product, process, or service by its trade name, trademark, manufacturer, or otherwise, does not necessarily constitute or imply its endorsement, recommendation, or favoring by the United States Government or any agency thereof, or the Regents of the University of California. The views and opinions of authors expressed herein do not necessarily state or reflect those of the United States Government or any agency thereof or the Regents of the University of California.

TABLE OF CONTENTS

ABSTRACT

I. INTRODUCTION ---------- 1

II. PRINCIPLES OF VAPORIZATION ---------- 2

A. Condensation and Vaporization ---------- 2

B. Equilibrium and Non-Equilibrium Vaporization ---------- 3

C. Langmuir Vaporization ---------- 4

D. Vaporization Enthalpies ---------- 8

III. SELECTED PHYSICAL CHEMICAL PROPERTIES OF ICE ---------- 10

A. Ice Vaporization Properties ---------- 10

B. Surface Properties of Ice ---------- 17

C. Bulk Properties of Ice ---------- 18

IV. EXPERIMENTAL PROCEDURES ---------- 25

A. Sample Preparation ---------- 25

B. Vaporization System ---------- 26

C. Gas Studies ---------- 27

D. Radiant Heating of the Sample Surface ---------- 27

V. EXPERIMENTAL RESULTS ---------- 29

A. Observations ---------- 29

B. Discussion ---------- 32

VI. ICE VAPORIZATION MECHANISM ---------- 37

VII. CONCLUSIONS ---------- 44

APPENDIX: THE LITERATURE OF ICE ---------- 47

ACKNOWLEDGEMENTS ---------- 49

REFERENCES ---------- 50

FIGURE CAPTIONS ---------- 54

VAPORIZATION MECHANISM OF ICE SINGLE CRYSTALS

John Gordon Davy

Inorganic Materials Research Division, Lawrence Radiation Laboratory
and Department of Chemistry
University of California, Berkeley, California

ABSTRACT

The kinetics of the vacuum sublimation of ice single crystals has been investigated by a vacuum microbalance technique in the temperature range -90° to -40°C. The vaporization coefficient $\alpha_v \equiv$ (observed vaporization rate) $\div$ (theoretical maximum rate) and the activation enthalpy of sublimation, ΔH_s^*, vary markedly with temperature in this range. Neither surface cooling nor gas-phase collisions can explain the observed behavior:

(1) At temperatures below about -85°C, $\alpha_v = 1$ and ΔH_s^* equals the thermodynamic enthalpy of sublimation ΔH_s°.

(2) Between about -85° and -60°C, α_v decreases slowly with increasing temperature, $\Delta H_s^* \lesssim \Delta H_s^\circ$.

(3) Between about -60° and -40°C, α_v decreases progressively more rapidly with increasing temperature and ΔH_s^* decreases to a high-temperature limiting value of $\simeq 1/2\ \Delta H_s^\circ$.

The effects of various experimental parameters such as crystal orientation, doping with impurities and adsorbed gases on the ice vaporization kinetics are presented and discussed: Neither grain boundaries nor crystalline orientation has a measurable effect on the rate. Ice doped with monovalent impurities was found to vaporize at steady-state rates that were uniformly lower over the entire temperature range of the study. Also, NH_3(gas) and HF(gas), present in the ambient at pressures ~10^{-3} to 10^{-2} torr, reduce and increase respectively the ice vaporization rate compared to the rate in vacuum.

The experimental results, along with previously reported physical-chemical properties of ice are used to arrive at a vaporization mechanism: Ice at equilibrium with the vapor has a uniform surface population of a highly mobile species assumed to be water molecules hydrogen-bonded to only one nearest neighbor. At sufficiently low temperatures, vaporization does not occur rapidly enough to alter this population. Sublimation at higher temperatures however, depletes the population to a progressively greater extent with increasing temperature. Thus the rate limiting step in vaporization, which is the desorption of the mobile water molecules at low temperatures, changes to their formation at high temperatures.

I. INTRODUCTION

A thorough study of the evaporation kinetics, along with other physical-chemical properties of a solid or liquid, may be used to arrive at a sequence of steps or mechanism by which molecules from the condensed phase enter into the vapor phase. Although the vaporization rates for many materials have been measured, vaporization mechanisms have been proposed for only a few, due to the lack of more detailed kinetic information. Thus, the vaporization rate of (polycrystalline) ice has been previously measured by several researchers (see Section III) but none has suggested a mechanism. Ice is an important material, and it is of interest both in its own right and as a prototype of all hydrogen-bonded compounds. I have measured the vacuum vaporization (sublimation) rate of ice in the temperature range -90° to -40°C. The samples included oriented single-crystal and polycrystalline ice, and ice doped with a variety of ionic impurities. In addition I have investigated the effects of different gases on the ice vaporization. The data accumulated in these studies, along with physical-chemical properties reported by others suggests a vaporization mechanism.

Before presenting the experimental procedure and results of the present investigation of ice vaporization, it will be desirable to review the existing information, both about the principles of vaporization studies and about various physical-chemical properties of ice..

II. PRINCIPLES OF VAPORIZATION*

The following discussion will consider only the vaporization of solids, although much could also be applied to liquids. It will be assumed that the only vapor molecules in the vicinity of the vaporizing surface are those of the solid being vaporized; that is, the vaporizing molecules are not scattered from any other kinds of molecules in the ambient vapor near the surface. (Experimentally, this means that the vaporization is carried out in vacuum. The mean free path of ambient molecules should be greater than the dimensions of the vaporizing surface, meaning that the pressures should be less than 10^{-2} torr). It is also assumed that there are no composition changes (association or decomposition) that occur in the process. I thus treat only the simple case of the vaporization for a one-component, two-phase system.

A. Condensation and Vaporization

Consider a crystal in the presence of its own vapor at pressure P. The vapor molecules impinge on the surface (see Fig. 1) with a flux $J_i = (2\pi mkT)^{-1/2} P$, where m is the mass of the vapor molecules, J_i has the dimensions of molecules per unit area per unit time, and k and T have their usual meaning. Of this impinging flux, a smaller flux J_{gc} will leave the gas phase and enter the crystal lattice (condense), and the remainder J_r will depart from the surface and return to the gas phase. Also departing from the surface is a flux of molecules J_{cg} that leaves the crystal and enters the gas phase (vaporizes). The total departing

*This section is not meant to be a comprehensive review of the subject; many excellent works are available. See for example, Somorjai and Lester (1967).

flux J_d is the sum of these two components. The net departing flux is the observable rate of vaporization $J_{obs} = J_d - J_i$.

At equilibrium, $J_{obs} = 0$, and $J_d = J_d^\circ = J_i^\circ$. (In this figure the superscript $^\circ$ is used to represent equilibrium). The equilibrium pressure is the saturation vapor pressure P_s.

In the figure are defined two parameters, α_c (condensation coefficient) and α_v (vaporization coefficient). At equilibrium, $\alpha_v = \alpha_c$; under any other conditions these coefficients may or may not be equal, but in the absence of information to the contrary it is usually assumed that they are equal. (Condensation coefficients are rarely measured when the net process occuring is vaporization, i.e., when $P < P_s$.)

By using these relationships, one can relate the observed vaporization rate J_{obs} to the vaporizing and condensing fluxes, and to pressure: $J_{obs} = J_{cg} - J_{gc} = (2\pi mkT)^{-1/2} (\alpha_v P_s - \alpha_c P)$. For a given temperature, the maximum possible value for the net vaporization rate is for the case $J_{gc} = 0$, $\alpha_v = 1$. This rate I will call J_{max}. Note that J_{max} is equal to the rate at which the surface is struck by molecules from the saturated vapor. Thus $J_{max} = (2\pi mkT)^{-1/2} P_s$.

B. Equilibrium and Non-Equilibrium Vaporization

Vaporization rates are measured under "equilibrium" and non-equilibrium conditions. "Equilibrium" measurements are those in which $J_i \simeq J_d$ so that J_{obs} is negligible by comparison. Stated alternately, the vapor above the solid is virtually saturated. The extreme of non-equilibrium vaporization occurs when $J_i = 0$ and $J_{obs} = J_d = J_{cg}$.

One example of the difference between these measurements is given in Fig 2 . In this example it is interesting to note that vaporization

is entirely analogous to the emission of photons by thermal radiation (Rossman and Yarwood, 1954). The substance in the "equilibrium" case is in a container which has only a small orifice through which vapor can escape, while the solid in the non-equilibrium case has a surface of known (projected) area exposed directly to the vacuum.

The "equilibrium" case (analogous to blackbody radiation) is called Knudsen vaporization. The orifice serves as a virtual source of molecules at the saturation vapor pressure P_s, which under ideal conditions can be calculated by measuring the rate at which molecules emerge from the orifice: $P_s = (2\pi mkT)^{1/2} J_{obs}$.

C. Langmuir Vaporization

"Equilibrium" measurements contain no information about kinetic processes occurring on or in the solid. (Analogously, emissivity cannot be measured by "equilibrium" techniques.) Kinetic processes are studied by the non-equilibrium method of Langmuir vaporization (analogous to gray-body radiation). Here under ideal conditions no vaporized molecule returns to the surface.

In Langmuir vaporization the observed rate is often below the maximum rate, as is indicated by Fig 1 . The ratio J_{obs}/J_{max} is the vaporization coefficient α_v. Since all the details of the vaporization mechanism are lumped into this one parameter, it is insufficient to merely record α_v values, which in general depend on temperature, incident flux, and various solid-state properties of the vaporizing surface. Some of the factors influencings J_{obs} are discussed under the following headings, and also in greater detail in Sections IV and V.

1. Gas-Phase Collisions Near the Surface (β-Effect)

Vaporizing molecules leave the surface in a distribution of angles, from normal to nearly parallel (Hirth and Pound, 1963). For high vapori-

zation rates, there is a finite probability that two vaporizing molecules will collide near the surface and that one of the two will be diverted back and strike the surface again. By the law of conservation of momentum, the maximum fraction of molecules that could after their last collision strike the surface is 1/2. This value applies to molecules with a pre-collision momentum normal to the surface equal to zero. For all other collisions, the fraction will be smaller.

The vaporization rate for which such collisions becomes appreciable can be estimated from knowing the pressure at which the mean free path of molecules in the saturated vapor becomes of the same magnitude as the dimensions of the vaporizing surface. (This sets a lower limit since the vaporizing flux has a net velocity, and thus a mean free path greater than the equilibrium vapor.)

One can define a parameter β as that fraction of the vaporizing molecules which escapes and does not return to the surface. $(1-\beta)$ is then the fraction which by colliding with other vaporizing molecules does return. By neglecting the net momentum of the vapor flux normal to the surface, one obtains an extreme lower limit for β of 1/2, but as has been argued, the true lower limit may be considerably above this (Burrows, 1954, 1957). The β-effect is considered further in Section V.

2. Surface Cooling

Another phenomenon which can cause J_{obs} to be too low at high vaporization rates is surface cooling. Since vaporization is an endothermic reaction the vaporizing surface may be cooler than the bulk if it relies on solid-state thermal conduction to supply the heat of vaporization. This is a problem that is frequently encountered in vaporization studies, but it can be overcome by supplying heat radiantly directly to the vapori-

zing surfaces so that temperature gradients do not occur. If this is not done, it is necessary to restrict vaporization studies to a temperature range in which the evaporation rates are low enough that the solid-state heat flow does not produce a significant temperature gradient. The surface cooling problem is discussed in greater detail in Section IV.

3. Impurities

Impurities in the bulk or on the surface may also affect J_{obs}. In addition to having a possible chemical influence on the host solid, they may also physically block a certain fraction of the vaporizing surface and thus lower the rate. On the other hand, it is important to recognize that many potential contaminants may have no effect whatever on the steady-state vaporization rate because they are efficiently removed by vaporizing molecules. Deamer and Branton (1967) showed that on ice a complete monolayer of stearic acid was unable to permanently retard the vaporization, even at the relatively low temperature of -100°C, where the rate at which the surface recedes is about 1200Å per minute. In ten minutes approximately one-half of the monolayer had been broken up and removed with the vaporizing water molecules.

4. Gas Effects

For most cases it is reasonable to assume that gaseous impurities impinging on the surface at a rate J_i will have no effect on J_{obs} as long as $J_i \ll J_{obs}$. However, if $J_i \sim J_{obs}$, then it is possible that a physical or chemical influence on J_{obs} will be observed. An observed gas effect i.e., a change in J_{obs} may be of value in arriving at a vaporization mechanism.

5. Use of Single Crystals

The vaporization rate of a material may depend on which crystal face is vaporizing, as well as on crystal defects such as grain boundaries and dislocations. For a well-defined study, it is necessary to use oriented single crystals, at least until it can be demonstrated that orientation and grain boundaries have no effect on the vaporization of the solid being investigated.

6. Surface Roughness

J_{obs} is calculated from the observed weight loss and a geometrical or projected area. Many materials develop a rough surface during vaporization and so it is necessary to consider the effect on J_{obs} when the true surface area exceeds the projected area. It might be expected that a sample with a rough surface may vaporize more rapidly than one with a smooth surface, and in general this is true, but the following points are important to consider:

(1) If $\alpha_v = 1$, the vaporization rate per unit of projected area is entirely independent of true surface area. This follows from the thermodynamic condition that the flux across any plane cannot exceed the flux corresponding to the saturation vapor pressure. Melville (1936) shows that if $\alpha_v = \alpha_c = 1$, the initially larger flux from a rough surface is reduced to the smooth-surface value because molecules vaporizing from one part of the surface can strike another part of the surface and recondense.

(2) Only in the limit of a recondensation rate of zero (α_v, $\alpha_c \rightarrow 0$) does the vaporization rate become proportional to true surface area (Rosenblatt, 1963).

(3) For a single crystal face, the steady-state surface area may not be an independent variable. That is, a sample with an initially

smooth face may become rough and a sample with an artifically roughened surface may become smoother, and J_{obs} may not take on a steady value until this occurs.

(4) The increase in true surface area observed on most evaporating single crystals is less than a factor of two over the projected area, and in view of the previous three points it may be asserted that J_{obs} takes an intermediate value between J_{cg} (flat surface) and J_{max}.

D. Vaporization Enthalpies

So far the discussion has been for one temperature. By varying the temperature it is possible to study the energetics of the vaporization process. The Clausius-Clapeyron equation relates the temperature dependence of the saturation vapor pressure and the standard* enthalpy of sublimation, ΔH_s° :

$$\frac{d\ln P_s}{d(1/T)} = \frac{-\Delta H_s^\circ}{R},$$

where R is the gas constant. Thus a plot of log P_s vs T^{-1} gives a line with a slope of

$$\frac{-\Delta H_s^\circ}{2.3R}$$

see Fig. 3. If instead, log J_{max} vs T^{-1} is plotted, then since $J_{max} = P_s (2\pi mkT)^{-1/2}$, the line will have a slope

$$\frac{-\Delta H_s^\circ}{2.3R} + \frac{T}{4.6}.$$

---

*If follows from the assumptions of the Clausius-Clapeyron treatment that ΔH_s, the true enthalpy of sublimation at pressure P_s, is the same as ΔH_s°, the standard enthalpy of sublimation, where the superscript $^\circ$ denotes solid and gas in their standard states. The subscript s is used with ΔH to denote sublimation, for although throughout this discussion the term vaporization is used, it is the enthalpy of sublimation (fusion plus vaporization) which is required.

The second term is always less than 5% of the first term and is often ignored. Also, ΔH_s° ordinarily varies only slowly with temperature. Thus such plots are usually drawn as a straight line.

If we now treat the kinetic data in the same manner as the equilibrium data, i.e., if $\log J_{obs}$ instead of $\log J_{max}$ is plotted, then the slope of the line will be

$$\frac{-\Delta H_s^*}{2.3R} + \frac{T}{4.6},$$

where ΔH_s^* can be called the "experimental activation enthalpy of sublimation", by analogy with ΔH_s°, the equilibrium standard enthalpy of sublimation.*

Although it is necessary that $J_{obs} \leq J_{max}$, the only restriction on ΔH_s^* is that it be positive. It is not necessary that it have a constant or near-constant value; in fact the experimental activation enthalpy and its temperature dependence can be important clues to the vaporization mechanism, as will be discussed in Section VI.

It is worth mentioning that ΔH_s^* could also be obtained by alternate methods. Let P' be defined as the apparent saturation vapor pressure: $P' \equiv \alpha_v P_s$. Then

$$\frac{d \log P'}{d(1/T)} = \frac{-\Delta H_s^*}{2.3R},$$

and

$$\frac{d \log \alpha_v}{d(1/T)} = \frac{\Delta H_s^\circ - \Delta H_s^*}{2.3R}$$

so that a plot of $\log P'$ or $\log \alpha_v$ vs T^{-1} would yield ΔH_s^*.

---

*It is important to note that ΔH_s^* is an experimentally determined parameter, and is different from $\Delta H^\ddagger$, the activation enthalpy employed in absolute reaction rate theory. This point will be discussed further in Section VI.

III. SELECTED PHYSICAL-CHEMICAL PROPERTIES OF ICE

The literature available on ice is voluminous and covers a wide range of topics, including glaciology and reports on the suitability of ice for airplane runways. Out of this wealth of information, I will present in this section only a few topics that will be of greatest value in connection with ice vaporization and its mechanism. Ice vaporization properties, surface properties, and bulk properties are covered in Parts A, B, and C. In addition, I present in the Appendix a brief discussion of various books and collected works on ice topics of physical-chemical interest.

A. Ice Vaporization Properties

1. The Saturation Vapor Pressure of Ice

Although many physical-chemical properties of ice are presently under intensive study, the saturation vapor pressure is one property which seems to be fairly well established.* However, because much of the information is published in journals that may not be readily available, I review here in some detail the work which has been reported.

The last reported measurement of the saturation vapor pressure of ordinary ice was carried out by Weber in Leyden in 1915. Weber used a number of pressure gauges; he made his lowest temperature measurements (to -100°C) with an absolute manometer. No study of the vapor pressure of ice by the Knudsen technique has ever been reported.

The absence of recent measurements does not mean that accurate values are not available, since the saturation vapor pressure is calculable at any temperature using thermodynamic functions by an integration of the

*Measurements and calculations for various isotopic ices have appeared recently - see for example Van Hook (1968).

Clausius-Clapeyron equation. In order to calculate the saturation vapor pressure P_1 at temperature T_1, it is only necessary to know its value P_0 at temperature T_0, and the enthalpy of sublimation as a function of temperature:

$$\log (P_1/P_0) = \frac{1}{2.3R} \int_{T_0}^{T_1} \frac{\Delta H_s^\circ}{T^2} dT. \qquad (1)$$

$$\log (P_1/P_0) = \frac{1}{2.3R} \left[\Delta H_{s,T_0} \left(\frac{1}{T_0} - \frac{1}{T_1} \right) + \int_{T_0}^{T_1} \frac{dT}{T^2} \left(\int_T^{T_0} C_{ps}\, dT + \int_{T_0}^{T} C_{pg}\, dT \right) \right] \qquad (2)$$

where $\Delta H^\circ_{s,T_0}$ is the standard enthalpy of sublimation at temperature T_0, and C_{ps} and C_{pg} are the constant-pressure heat capacities of solid and gas.

The saturation vapor pressure of ice is best known at the triple point: $T_0 = 273.16°K$, $P_0 = 4.579$ torr. The standard enthalpies of sublimation at the triple point and at absoulte zero are given by Eisenberg and Kauzmann (1969) to five places: $\Delta H^\circ_s = 12{,}203$ and $11{,}316$ kcal mole,$^{-1}$ respectively. Kelley (1935) reports $\Delta H^\circ_s = 11{,}260 + 7.66T - 15.6\times10^{-3}T^2 + 0.446\times10^{-6}T^3$, which yields $\Delta H^\circ_{s,273.16} = 12{,}197$ kcal mole. The values given by the two authors are thus quite close at the triple point but somewhat farther apart at absolute zero. Kelley also gives analytical expressions in T for the heat capacities of solid and gas.

The saturation vapor pressure is given as a function of temperature by an expression of the form $\log_{10}(P_1/P_0) = \theta\,(1/273.16 - 1/T_1) + f(T)$. θ is a fixed sublimation enthalpy divided by 2.3R and has dimensions of temperature. The expression f(T) represents all other terms. For ease of calculation, an expression in which f(T) = 0 can be used; for temperatures near 0°C it is desirable for this purpose to use $H^\circ_{s,273.16}$ to calculate θ. Using the enthalpy value given by Eisenberg and Kauzmann,

θ= 2,667°K which gives the simplified expression $\log p_1 = 2667 (1/273.16 - 1/T_1) - \log p_0 = 10.425 - 2667/T_1$. For temperatures above -100°C, the saturation vapor pressure of ice calculated by this equation gives values that differ by less than 1% from the best tabulated values (Smithsonian, see below).

Equations with a larger number of terms have been given by three previous authors;(1) E. W. Washburn (1924), who reported the details of his caluclations in the Monthly Weather Review. Washburn used Eq. (2), first assuming C_{ps} and C_{pg} were constant and then modifying the values of θ and the heat capacity terms to fit the experimental saturation vapor pressure data. His value for θ is 2445.5646°K.* The values (in torr) are given in tenth-degree increments from 0° to -30°C and in one-degree increments to -100°C in the International Critical Tables (1929), but with 3-place accuracy only to -74°C. They are also given in Dorsey (1940) and in editions of the Chemical Rubber Company Handbook. (2) S. Dushman (1962) uses Eq. (1) and Kelley's expression for ΔH°_s; he tabulates the saturation vapor pressure to three places in ten-degree increments to -140°C. Because the term in T^{-1} is based on $\Delta H^\circ_{s,0}$, the value for θ is smaller (θ=2461°K) and it is necessary to include at least the terms in T and T^2 for computations (the calculated saturation vapor pressure is about 2-1/2 times too high at -100°C if these terms are neglected.) (3) The most accurate saturation vapor pressure data for ice and the most extensive tabulations come from work by Goff (1942) and Goff and Gratch (1946). These calculations were based on Eq. (2), with corrections not only for the heat capacities and their temperature dependences, but also for gas nonideality. (The volume correction for the solid was found to be entirely

*A simpler formula based on Washburn's data is proposed by Whipple (1927). The value of θ from this proposal is 2717°K.

negligible.) The θ values from their expressions are 2689°K and 2668°K. Their calculations were carried out in engineering units, and tabulated (Goff-Gratch) in psi and inches of mercury, along with other thermodynamic properties, in one-degree increments between 32°F and -160°F.

The saturation vapor pressure of ice is tabulated most extensively in the Smithsonian Meteorological Tables (List, 1951), in millibars, in tenth-degree increments from 0° to -100°C. According to a note in this book, the tabulated values are derived from Goff and Gratch (1946). However, the expression given in the Smithsonian Tables differs from that of Goff and Gratch and has a θ of 2485°K. In any case, the Smithsonian tabulation is so extensive that calculation from analytical expressions should rarely, if ever, be necessary.

2. Previous Measurements of Ice Vaporization Rates

The results of all previous investigations of the vaporization rate of (polycrystalline) ice is given in Fig. 4 , along with the results of the present study, which will be discussed in Section V. This figure is a plot of the logarithm of the vaporization rates vs. reciprocal temperature, as discussed in Section II. Except as noted the ice samples used by these workers were prepared by degassing and then freezing distilled water under vacuum just prior to performing their measurements.

(1) Delaney et al., (1964) used a non-steady-state technique to obtain a value $\alpha_v = 0.0144 \pm .0020$ for temperatures between -13° and -2°C, and for an incident flux J_i nearly equal to the departing flux J_d, i.e., $J_i/J_d \lesssim 1$. The two lines marked D in Fig. 4 were obtained by plotting values of $\alpha_v J_{max}$ for the two runs they report. Note that the predicted rates at these temperatures are near those observed between -50° and -40°C.

However, since α_v may depend on J_i/J_d, it is not certain that these results are directly comparable to the results from free vaporization studies (i.e., $J_i/J_d \ll 1$).

(2) Baranaev (1946) used the method of Alty (1937) to obtain the vaporization rate at -48°, -46°, and -44°C. A straight line fitted to these values is marked B in Fig. 4 . Although Baranaev calculated his results assuming that $J_i \ll J_d$, the low values ($\bar{\alpha}_v = 0.068$) obtained make his assumption doubtful. Another possibility is that the temperature measurements were in error due to thermal gradients in the sample. Baranaev does not state whether the water from which he froze his sample had been degassed.

(3) Strickland-Constable and Bruce (1954) used a balance technique with a liquid-air cooled condenser subtending part of the solid angle above the vaporizing surface. Apparently they did not degas their water prior to freezing. Their results, for -55° to -50°C, are shown by the line labelled SCB. These workers considered gas-phase collisions (β-effect) and reported a value $\gamma \equiv \alpha_v\beta$; they suggest that $\alpha_v = 1$ and $\gamma = \beta$. (The values they report for γ are too low; only their values of J_{obs} were used to plot their results in Fig. 4).

(4) Kramers and Stemerding (1951) also used a balance technique and a plane-parallel condenser, which they positioned at distances between 12 and 44 mm from the vaporizing surface. They experienced difficulty maintaining a uniform surface temperature. Because of the large scatter of their results -α_v between 0.5 and 1.4-only their temperature range (-60° to -40°C) is indicated (between arrows marked KS). For these studies, the condenser temperature was never more than 12°C below the

temperature of the vaporizing surface. This resulted in a non-negligible flux incident on the vaporizing surface, which they took into account. Within the accuracy of their results there was no apparent tendency for the incident flux to lower α_v; in fact they concluded that $\alpha_v = 1$ over their temperature range and that departures of J_{obs} below the calculated rate were due to gas-phase collisions and wall effects.

(5) Tschudin (1946) used an electrical balance and a liquid-air cooled condenser positioned a few millimeters over the vaporizing surface. After making 43 rate measurements between -85°C and -60°C, he concluded that $\alpha_v = 0.94 \pm 0.06$ over the temperature range (shown in Fig. 4 between arrows marked T_s).

(6) Koros et al. (1966) measured the condensation coefficient of water molecules on ice using a molecular beam apparatus. In the temperature range -140° to -115°C, they report a value for α_v of 0.83 ± 0.15. Because these results are for condensation rather than vaporization, they are not shown.

(7) Ison and Iwai (1969) measured a condensation coefficient of about 0.06 between -50° and -80°C; below this temperature they observed α_c to increase to about 0.5 at -110°C.

3. Association of Water Molecules in the Vapor

In Section II, the discussion of vaporization was limited to one vapor species: the monomer molecule with the same composition as that of the solid. For ice vaporization, this means that the possibility of the presence of water molecule polymers such as the dimer $(H_2O)_2$ in the vapor is ignored. I will try to show here the polymers can be expected to make up only an insignificant part of the total water-vapor composition i.e, water vapor is predominantly monomeric, and the restriction imposed in Section II is therefore justifiable.

Eisenberg and Kauzmann (1969) devote most of one chapter of their book to an analysis of the forces between water molecules in the vapor phase. They observe that hydrogen bonding, which is of great importance in the condensed phases of water, is rare or non-existent between water molecules in the vapor.*

Eisenberg and Hauzmann discuss various attempts to look at the dimer concentration in water vapor; they present a calculation by Rowlinson from which it is possible to compute the dimer/monomer molecular ratio in the saturated vapor: it rises with temperature, but is only about 5×10^{-4} at 0°C. More recently, Milne and Greene (1967) and Greene et al. (1969) have carried out mass-spectrometric sampling of near-saturated water vapor, obtaining a dimer/monomer ratio varying between 3×10^{-4} at 0°C and 1.6×10^{-2} at 100°C. No measurements of the dimer concentration in water vapor at temperatures below 0°C have been reported. While it is possible that the dimer/monomer ratio for free vaporization of ice is somewhat different than for saturated water vapor, it would need to be at least two orders of magnitude higher in order to be an important feature of the vaporization mechanism.

4. Possible Charging of the Ice Surface During Vaporization

Various electrical charging mechanisms for ice, water, and water vapor have been proposed to explain thunderstorm electricity. However, Cross and Speare (1969) have shown that for ice vaporization at temperatures near 0°C under a vacuum of 0.5 torr, the largest current density generated was of the same magnitude as their experimental uncertainty ($\sim10^{-15}$ amp cm^{-2}).

*In contrast, the concentration of hydrogen-bonded dimers and ring-hexamers in saturated HF vapor can be calculated from data in Franck and Meyer (1959) to exceed the concentration of the monomer, at least for temperatures below the boiling point (19°C). Little is known about polymerization in NH_3 vapor.

Apparently, thunderstorm charging effects must involve ambient conditions which are different than those established during vacuum vaporization of ice.

B. Surface Properties of Ice

1. Surface Morphology of Vaporizing Ice

Recent microscopic studies of the vaporizing ice surface have shown that it exhibits a variety of interesting features. One such feature, which can develop at temperatures from -10° down to -50°C (and possibly lower) is fibers, or "whiskers", seen both by optical microscopy (de Micheli and Licenblat, 1967; Lykov et al., 1968), and scanning electron microscopy (Cross, 1969). These whiskers appear to form preferentially at cracks and grain boundaries. Examination by transmission electron microscopy of replicas vapor-deposited on ice samples vaporizing at temperatures between -110°C and -60°C (see Fig. 5) have shown features which may be related to these whiskers (Davy and Branton, 1970). This study investigated the ice surface morphology as a function of temperature, extent of vaporization and crystal orientation. The results can be summarized as follows: (1) Flat-bottomed etch pits about one micron in diameter develop, grow larger and shallower, and finally disappear. These etch pits are probably due to surface dislocations introduced during surface preparation by cleavage. The density of bulk dislocations in the ice appears to be very small. (2) At temperatures below -90°C, bumps or asperities about 300Å in diameter develop on the subliming surface. Their density is about 2×10^{10} cm^{-2}, and does not vary appreciably with temperature, extent of vaporization orientation, or sample purity. It was not possible to attribute these asperities to impurities, but they may be related to the growth of whiskers that have been observed at higher temperatures.

(3) At temperatures above -90°C, the surface became progressively rougher, and above -85°C, it was not possible to produce a continuous replica. This roughness may be produced by whiskers too fragile to be preserved by the replication technique. It is important that the roughness develops at the temperatures for which α_v begins to depart from unity.

2. "Liquid-like Layer" on Ice Surface

The nature of the ice surface has been a matter of active interest since the time of Faraday, who in 1850 proposed that ice at temperatures near the melting point was covered by a liquid-like film. The bibliography now available on this one topic alone is long, and I will mention here only the review by Jellinek (1967). The liquid-like film was postulated to explain the ease with which two pieces of ice stick together. This property was termed "regelation" by Tyndall, but is now explained as sintering. This sintering is attributable to surface molecules of high surface mobility, and occurs at measurable speed down to -25°C or below in a saturated atmosphere, but only to -3°C in a dry atmosphere. For present purposes, this is one of the most important characteristics of the ice surface: the population of the highly mobile species (liquid-like or other) is observed to be greatly reduced under dry (high net vaporization) conditions.

C. Bulk Properties of Ice

1. Structure

Under ordinary conditions ice has a hexagonal crystal structure commonly called ice I. The structure of the oxygen sublattice of ice I was determined by Bragg in 1922 (see Figs. 6 and 7) but the positions of the hydrogens were in question until 1957, when they determined by neutron diffraction of D_2O ice.* The results confirmed the hypothesis that

*For a stereo view of the ice lattice, including hydrogen positions, see Hamilton and Ibers (1968).

Pauling had made earlier (1935):

(1) In ice each oxygen atom has two hydrogen atoms attached to it at distances of about 0.95Å, forming a water molecule, the HOH angle being about 105° as in the gas molecule.

(2) Each water molecule is oriented so that its two hydrogen atoms are directed approximately toward two of the four oxygen atoms which surround it tetrahedrally, forming hydrogen bonds.

(3) The orientations of adjacent water molecules are such that only one hydrogen atom lies approximately along each oxygen-oxygen axis.

(4) Under ordinary conditions the interaction of non-adjacent molecules is not such as to appreciably stabilize any one of the many configurations satisfying the preceding conditions with reference to the others.

Recent information has modified these assumptions only slightly: In H_2O ice, the hydrogen is 0.99Å from the closer oxygen and the HOH angle is very close to tetrahedral (109-1/2°). Upon vaporization the bond angle for the vapor molecule changes to 105°. Also, assumptions 1 and 3 are occassionally violated by defects (discussed in division 2 below).

Bridgman demonstrated the existence of a number of high-pressure polymorphs of ice and recently their structures have been determined. However, none of these are stable at pressures of less than 2000 atmospheres, and will not be discussed further. An amorphous (or microcrystalline) form and a cubic form of ice have been prepared by vapor-depositing water vapor on a cold substrate. They transform to ordinary hexagonal ice I upon warming above about -100°C.

2. Defects (Gross, 1968; Kröger, 1964)

In 1951 Bjerrum proposed that ice might contain two basic types of defects: ionic and orientational. The ionic defect is a violation of

Pauling's assumption 1: some oxygens have one or three hydrogen atoms attached and so are HO^- and H_3O^+ ions. These ions are present in concentrations of about 10^{12} cm^{-3} each at -10°C, compared to an H_2O molecule concentration of 3×10^{22} cm^{-3}. (This value for the ionic concentration, which is considerably higher than that given in the review articles listed in the Appendix, is based on recent measurements of the conductivity (Wörz and Cole, 1969) and ion mobility (Heinmets, 1960). The energy to form an ion pair is about 23 kcal $mole^{-1}$, or nearly twice the enthalpy of vaporization. By way of comparison, the energy of a hydrogen bond is much smaller. Various estimates have been made for the hydrogen bond energy (Pimentel and McClellan, 1960), but for present purposes it will be satisfactory to assign a value of one-half of the enthalpy of sublimation to each bond (6.1 kcal $mole^{-1}$) since vaporization of one mole of ice requires breaking two moles of bonds.

The orientational defect has come to be termed a Bjerrum defect; it is a violation of Pauling's assumption 3. A Bjerrum defect is formed when a molecule rotates 120° about one bond to leave one oxygen-oxygen axis without a hydrogen link (a vacant bond) and another with two protons along it (a double-proton bond). These defects are now known as L and D defects respectively ("Leerstelle" and "Doppelbesetzung") after the usage of Steinemann and Gränicher (1957). The molecule which rotates to form the D-L defect pair may of course rotate back to annihilate it, but if an adjacent molecule rotates first, then the L and D defects become separated before they are annihilated and by successive molecular rotations they can independently migrate through the crystal lattice. The L+D defect concentration at -10°C is about 10^{16} cm^{-3} (0.3 ppm) and the energy to

form a defect pair is 15.6 kcal $mole^{-1}$ (Gross, 1968). The activation energy for diffusion of defects is: ions, zero (due to tunneling); Bjerrum 5.4 kcal $mole^{-1}$. If we assume that the Bjerrum defect concentration at the surface is equal to that in the bulk, it is possible to calculate the rate at which a given molecule is visited by a Bjerrum defect, and to compare that value with the vaporization rate in appropriate units. The result is that in the length of time that a given layer is exposed on the surface, less than 0.05% of the molecules in the layer will be visited by a valence defect. Consequently, Bjerrum defects are not likely to play a major role in the vaporization of pure ice, unless they are present in much higher concentrations at the surface than in the bulk.

If the concentration of one type (L, say) of Bjerrum defects were increased by a factor of 10^3 to 10^4, by doping the ice with HF, it might be possible to study the defect effect on the vaporization rate. Because HF with one proton is substituted in the lattice for H_2O (with 2), the L defect concentration is approximately equal to the concentration of HF. (The ionization constants for HF and NH_3 in ice are very small). The concentration of L defects in pure ice at -60°C is about 10 ppb; a 10^4 increase would require HF doping at 100 ppm, and this is about the limit of solubility. Hence any Bjerrum-defect of HF dissolved in ice is likely to be small. An equivalent situation holds for NH_3.

Ionic and Bjerrum defects do account for the electrical properties of ice -- protons have been shown to be the major charge carrier, and the possibility of Bjerrum rotation is required to explain the high static dielectric constant. However, recent experiments indicate that extreme care is necessary during electrical measurements since electrode space-charge effects, surface conductivity, and particularly, charged impurities

make the investigation difficult. Consequently, reports on the electrical properties of ice must be read and interpreted with care. The activation energy for electrical conductivity is in doubt.

Lattice vacancies and interstitials have not been studied as extensively as the other types of defects but it is believed that self-diffusion of H_2O molecules occurs interstitially via the open lattice, possibly in conjunction with an orientational defect. Onsager and Runnels (1969) have published an analysis of several rate processes in ice: the activation energy is between 13 and 16 kcal mole^{-1} for self-diffusion and for dielectric, elastic and spin-lattice relaxation.

Dislocations, which have been observed to influence the vaporization rate of NaCl, are present in unstrained ice in very low concentrations (~1 cm^{-2}, Webb and Hayes (1967); ~10^4 cm^{-2}, Fukuda and Higashi (1969)); they appear to play no role in its vaporization.

3. Growing and Doping*

It is remarkable that while water is referred to as a "universal solvent", the solubility of all materials except one in ice is on the order of parts per million or less. The sole exception is NH_4F, which is isoelectronic with two H_2O molecules and has the same crystal structure as ice. The solidus line for the system H_2O- NH_4F indicates a solubility of NH_4F in ice of 7 mole percent at the eutectic temperature of -28°C. (Labowitz and Westrum, 1961). However, large, clear single crystals of NH_4F-doped ice are obtainable only for concentrations below about 0.1 mole percent; for NH_4OH and HF, and limit is about 0.01 mole

*Except as otherwise noted, information in this section comes from Gross (1968).

percent (100 ppm)(Jaccard and Levi, 1961). (NH_4F is not incorporated stoichiometrically: more HF than NH_3 goes into the lattice). The solubility of most other dopants is unknown, but they are likely to be very low: HCl and NaOH dissolve only to about 0.1 ppm (Young and Salomon, 1968; Kelley and Salomon, 1969).

On the other hand, it is not easy to grow ice of high purity, and extremely small amounts of impurity ($\sim 10^{13}$ cm^{-3} or < 1 ppb of HF) may alter such properties as the dielectric relaxation activation energy. (Gross 1968). Barnaal and Lowe (1968) observed (for temperatures below -50°C) that the spin-lattice relaxation time T_1 in ice was increased with each zone-refining pass up to the tenth. Jaccard and Levi found that growth rates in excess of 0.5μ sec^{-1} led to inhomogeneities in the distribution of impurities in the ice lattice.

During the growth of ice from a solution containing electrolytes ($\geq 10^{-6}$M) an electrical potential between ince and solution builds up due to selective ion incorporation. This phenomenon (the Workman-Reynolds effect) was reported in 1950. However, most of the investigation of the growth of pure and doped ice has been carried out in the last decade, and because of the complexity of the subject and the discordance of many of the reported results, much remains to be understood.

4. Mechanical Properties

Jones and Glen (1969) found that ice doped with HF in concentrations up to 67 ppm was softer than pure ice, while ice doped with NH_3 appeared to be harder than pure ice. They attribute the softening to L defects, and suggested that D-defects did not cause softening either because D defects

produced by NH_3 were not mobile (trapped by NH_3), or because D-defects were immobilized by dislocations. If D-defects are not mobile and cannot cause softening in the manner of L-defects, then the net result of NH_3 doping is a reduction in the mobile defect concentration below the pure ice value and a consequent hardening.

5. Optical Properties

Ice is transparent to visible light and optically active. The crystalline c-axis (vertical direction in Fig. 6) is the optic axis. By examining an ice sample between crossed polaroids, grain boundaries are visible and crystalline orientation can be determined. The experimental techniques are described briefly in Section III, and more extensively in Wood (1964).

IV. EXPERIMENTAL PROCEDURES

In the system to be described, Langmuir vaporization rates are obtained by using a vacuum microbalance to monitor the weight of the ice sample.

A. Sample Preparation

1. Jona-Scherrer (Doped and Undoped) Single Crystals

As mentioned in Section II, it is desirable for Langmuir vaporization to use single crystals of known orientation, at least until it can be demonstrated that neither orientation nor the presence of grain boundaries affect J_{obs}. The technique used to prepare single crystals of ice for Langmuir vaporization, including one method of growth that was used, is shown in Fig. 8. The preparation was carried out in a walk-in freezer maintained at -10°C. (a) Large pieces of very clear ice are obtained from distilled water by slow growth in a 600 ml beaker, after the method of Jona and Scherrer (1952). (b) Because ice is transparent and optically active, a suitable single crystal can be readily selected by using polarized light (Wood, 1964) and cutting away from its neighbors. (c) The orientation of the crystal is determined in a polarizing microscope. (d) The desired sample has one exposed face of known surface area, so an aluminum sleeve (5/16" dia., 1/4" long, 0.005" wall thickness) is melted down into the ice and the excess is trimmed away with a knife. (e) A small thermocouple (0.003" copper-constantan) is "welded" to the back face of the crystal with a few drops of water and then this face is covered. The finished sample is ready to be suspended from the microbalance.

The same growth technique was used to produce "doped" samples: ice was grown from 0.1 and 0.01 M solutions of various acids, bases and salts to cause their incorporation into the ice lattice, since it was desired to

investigate the influence (if any) of these impurities on J_{obs}. For purposes of this discussion, the ice grown by the Jona-Scherrer method from distilled water will be called undoped.

2. High-Purity Samples

As another method of preparing ice (clear, but polycrystalline, with a grain size ~1 mm), distilled water with a conductivity below 10^{-6} $(\text{ohm-cm})^{-1}$ was degassed by pumping on it for several hours and then a portion was frozen (under vacuum) at a rate of about 10 μ/sec. These samples I call high-purity, because it is possible to keep their total contaminant level lower than in the so-called undoped samples.

B. Vaporization System

A block diagram of the system used to investigate the vaporization rate is shown in Fig. 9. J_{obs} is continuously monitored by electronically taking the time derivative of the sample weight measured by the microbalance. The measured noise levels are: balance: ± μg; differentiator, ±1 μg/min. Estimated errors for both balance and differentiator measurements are on the order of 1%. Further details of the system are given in Fig. 10 and in Davy (1970). An important feature of the system is that it is possible to obtain an accurate rate measurement that is both absolute and continuous, and that the sample temperature can be monitored simultaneously.

While the sample is being installed in the vacuum chamber, it must be partially surrounded by a miniature cold chamber which is removed just prior to pumpdown. (This cold chamber has one compartment which can be filled with a dry-ice acetone slurry, and a separate compartment for the sample).

Once pumpdown has started, it takes about five minutes for a steady-state temperature to be established; from that time on it is possible to

obtain vaporization rates. A new temperature is readily established by changing the heater control. If the radiant heater is off and the chamber is at room temperature, an ice sample's steady-state temperature is about -68°C. For lower temperatures, most of the chamber* can be chilled by liquid nitrogen; this takes about 15 minutes. The lowest ice sample temperature attainable in the cold chamber is about -90°C.

When the chamber is warm (room temperature), the ambient pressure P of water vapor is measured to be negligible compared to the effective saturation vapor pressure P' over the accessible temperature range; that is, $J_i < 0.05\ J_d$, so that $J_{obs} = J_{cg}$ to a satisfactory accuracy. When the chamber is cold, the ambient pressure is $\sim 10^{-6}$ torr, and the partial pressure of water vapor is presumably much smaller than this.

C. Gas Studies

For investigating the effects of various gases on J_{obs} it is desirable to introduce a gas into an isolated chamber to some arbitrary pressure and have that pressure remain reasonably fixed; this is readily accomplished by having the chamber cold. The walls act as an effective cryopump for water vapor and the background pressure rises at a negligible rate. Even for condensible gases such as HF and NH_3, the partial pressure remains fairly constant in the cold chamber, presumably because these gases first condense and then slowly re-evaporate from regions of the wall that are at an intermediate temperature.

D. Radiant Heating of the Sample Surface

It was mentioned in Section II that surface cooling can give values of J_{obs} that are too low; it is important, especially at the higher rates of vaporization in this study, that the true surface temperature be known.

---

*Up to, but not including the window and pump flanges.

Figure 11 gives the details of how this problem was solved. The sample is thermally isolated in a vacuum. Thus, if heat is supplied radiantly to the same surface that is absorbing it by vaporization, then steady-state temperature gradients within the solid should not be expected to occur, apart from the small heat losses indicated.

The figure gives estimated worst-case values for heat losses and the corresponding temperature difference (0.1°C) to be expected between front and back of the sample. Given for comparison is the rate of heat input (power) required to maintain the 0.5 cm^2 of ice surface at various temperatures, assuming $J_{cg} = J_{max}$.

The heater is a small coil of nichrome wire that had a measured impedance to the vapor flux of only about 1%. The heater control is a high-gain proportional controller capable of maintaining the sample temperature constant to within about 0.01°C.

The lowest sample temperature attainable has been discussed; it depends primarily on the success in shielding the sample from warm (room-temperature) surroundings. The high-temperature limit is set by success in supplying adequate radiant power to the sample surface. It must also be possible to make a steady-state rate measurement before the surface recedes far into the sleeve, since wall effects are not included in the Langmuir calculations. (It is possible to make corrections for small recessions.) Finally, it was observed that at the highest rates obtained (~35 mg cm^{-2} min^{-1}) the sample begain to swing due to the sizeable momentum transfer occurring. For the system described here, these three limitations all occurred at a temperature of about -40°C.

V. EXPERIMENTAL RESULTS

A. Observations

1. Steady-State Vaporization

The time required to reach a steady-state temperature and vaporization rate is on the order of thirty seconds to a few minutes. (Cooling to very low temperatures takes somewhat longer: ~ 1/2 hr. from -75° to -85°). Consequently, a large number of rate measurements can be carried out on a single sample in a matter of hours. (For some warm-chamber measurements, over a dozen experimental points were determined in under one-half hour.) I have found that for a given sample, the rate is a function only of temperature, and not of thermal history or of the amount of sample vaporized.*

For each ice sample, the values of J_{obs}, when plotted as the logarithm vs. T^{-1}, all lie quite accurately on a smooth curve. The uncertainty in the points of Figs. 12a an b is much smaller than the circles used to represent them. Each point represents a separate determination of the steady-state vaporization rate; the numbers beside the points give the order in which they were taken. The curves are drawn somewhat above the high-temperature points; this reflects a correction for the recession of the ice surface.

The results for five samples each of high-purity and of undoped ice are shown in Figs. 12c-d. The points shown are the averaged rates for

---

*On the basis of electron micrographs of the vaporizing ice surface (Davy and Branton, to be published), it appears that a steady-state surface morhpology develops by the time 1000A (~300 molecular layers) have sublimed, independent of temperature.

five samples, in increments of 10^{-4} in T^{-1}. The bars indicate the spread between the highest and lowest rates observed. The general shape of the vaporization curve is maintained for all samples including the doped samples (to be discussed below) with the exception of those doped with high concentrations of ammonia and ammonium fluoride, which will be discussed separately.

2. Fluctuations

For a given sample, the vaporization rate at steady state fluctuates about an average value. The magnitude of this fluctuation is small for the high-purity and the doped samples ($\leq \pm 5$ μg cm^{-2} min^{-1}) and large for the undoped samples ($\sim \pm 50$ μg cm^{-2} min^{-1}) and is independent of temperature. The fluctuation appears to be due to local variations in impurity content and will be discussed in Part B.

3. Reproducibility

There is a spread in observed vaporization rates for samples of the same type. For high-purity samples, the spread between highest and lowest rates observed at a given temperature is about 10%; for undoped samples, about 15%. Reproducibility for the doped samples is rather poor, due to the difficulties involved in growing single crystals of known and uniform doping.

4. Effect of Crystal Orientation and Grain Boundaries

The exposed surface for all five undoped samples reported was the c-face (c-axis $\perp$ to the surface.) Undoped samples that had other orientations (including c-axis $\parallel$ to surface) all had vaporization rates similar to that of the c-face samples within the accuracy of the experiments. Also, polycrystalline undoped samples had vaporization rates undistinguishable from those for the single crystals. Observation by optical microscope

of the surface after vaporization (and a subsequent exposure to air) showed, for all samples a surface macroscopically flat but roughened (like an orange skin). The polycrystalline samples showed no evidence of grain-boundary grooving.

5. Effect of Crystal-Lattice Impurities on Ice Vaporization Rate

The average vaporization rate for undoped ice is about 10% lower than for high-purity ice (see Fig. 12c); the rate for ice of even higher purity might be slightly higher. As mentioned before, the magnitude of rate fluctuations in the doped samples was much smaller than in the undoped samples.

Rate plots for doped samples have the same appearance as those for undoped samples, although there was in some cases a general reduction in the vaporization rate. The results for a number of monovalent impurities are summarized in Table I which gives the values for J_{doped}/J_{max}, evaluated at $T^{-1} = 4.8\ 10^{-3}\,{}^{\circ}K^{-1}(-65^{\circ}C)$. Because the results for ice doped with NH_4F differed from those for other dopants, a rate plot for several such samples is given in Fig. 13. The general effect of monovalent impurities appears to be a reduction in the vaporization rate. More reproducible results would require a sample growth method known to give uniform dopant concentrations.

Since NH_4F is so much more soluble in ice than other materials are, it is not surprising that its effect on the ice vaporization rate is more pronounced: α_v for ice grown from 1M NH_4F silution is about 0.06; the activation enthalpy is somewhat above the thermodynamic enthalpy of sublimation.

The effect of one trivalent impurity was investigated; the vaporization rate of ice grown from a saturated solution of $Cr(NO_3)_3$ was measured. The vaporization behavior was indistinguishable from that of an undoped sample, and for this ice, there was no suppression of the rate fluctuation.

Of special interest is the behavior of the sample from 1M NH_4OH, which was quick frozen over dry ice. The result was a sluch of small ice

grains coated with aqueous ammonia (eutectic temperature -120°C). When this sample was placed in the vaporization chamber, its first values of J_{obs} were well above J_{max} (see Fig. 14). It eventually reached a steady-state rate with $\alpha_v \sim 0.9$ over the temperature range investigated. (The apparent curvature in the rate plot at higher temperatures is due to surface recession.) The significance of these observations will be discussed in Part B below.

6. Effect of Gases on Ice Vaporization Rate

The influence of the following gases on J_{obs} was investigated: H_2, He, N_2, O_2, CO_2, $C_2H_2F_4$, C_2F_6, H_2S, NH_3, HCl and HF. The gas was admitted to a pressure of about 10^{-3} torr while the temperature of the ice sample was such that its saturation vapor pressure was about 5×10^{-3} torr. Thus, the vaporization flux and the gas flux incident on the surface were of similar magnitude.

All of these gases except NH_3, HCl and HF caused a slight decrease in the vaporization rate attributable to the small physical effect of gas-phase collisions near the vaporizing surface.

The effect of NH_3 was a considerably greater reduction in the vaporization rate. HCl did not decrease the rate below the rate in the vacuum, and HF increased the rate.

These three gases and N_2 as a reference gas were investigated further to find the temperature and pressure dependence of J_{gas}/J_{vac} and the results are given in Fig. 15.

B. Discussion

The observations presented in Part A are discussed below; those of greatest value in choosing a vaporization mechanism are discussed further in Section VI.

1. Vaporization Rate and Activation Enthalpy

The most important feature of the vaporization process of ice is the marked curvature in the plot of log J_{obs} vs T^{-1}, implying a large change in the experimental activation enthalpy ΔH_s^* within the temperature range studied (see Figs. 12c and d). This feature has never before been reported in vaporization rate studies of ice.

It will be noted that the asymptotic behavior at low temperatures is for $\Delta H_s^* \rightarrow \Delta H_s^\circ$, and for the high-purity samples, $\alpha_v \rightarrow 1$. The high-temperature asymptotic behavior is more difficult to determine with certainty; rate measurements up to -35° or -30°C would be of great value. An argument will be given in the next section that the most reasonable high-temperature limiting value for ΔH_s^* is $1/2\ \Delta H_s^\circ$, as indicated in Figs. 12c and d.

Since the curvature is observed at relatively high rates, it is necessary to show that neither surface cooling nor gas-phase collisions (the β-effect) can suitable account for the observed behavior. At the highest rates, the error in the temperature measurement necessary to give $\alpha_v = 1$ (i.e, $J_{obs} = J_{max}$) is about 7°C. Because of the heating method employed, and as can be concluded from the results obtained for ice frozen from 1M NH_4OH (see below) such an error seems very unlikely.

It might be argued that since the lowest measured value for α_v is about 0.5, that in fact $\alpha_v = 1$, and $\beta = 1/2$. However, even in the absence of exact calculations, it is possible, based on the mean free path of water molecules in the saturated vapor (see Fig. 16a) to plot the predicted qualitative behavior for ice if α_v were indeed unity over the entire temperature range (Fig. 16b). For the sample size used (0.5 cm^2), β might be expected to depart appreciably from unity when the mean free

path is ~1-2 cm, and to reach its minimum value when the mean free path is ~1 mm. At this minimum value the slope of the predicted rate J_{pred} will be the same as for $\beta = 1$. Stated another way, ΔH_s^* (pred) will equal ΔH_s° except in the intermediate temperature region where β is changing.

Since the observed high-temperatures limiting value for ΔH_s^* is much less than ΔH_s°, the lowering of α_v cannot be entirely attributed to the β-effect. The true α_v may be somewhat higher, but the β-effect (which lowers α_v) is offset by surface roughening (which raises α_v).

2. Impurity effects

It seems likely that the fluctuations in the observed rate for the undoped samples are due to an uncontrolled incorporation of trace amounts of impurity in the samples during growth. (The magnitude of the fluctuation -- ± 50 μg cm^{-2} min^{-1}-- is unimportant when compared to vaporization rates above about -75°C but it did make it difficult to collect reliable data below that temperature.)

It is of interest that the magnitude of the fluctuation was reduced at least tenfold, both by growing samples of higher purity and by deliberate doping. If the high rate fluctuations for the undoped samples are due to local variations in the type and concentration of impurities, then either an overall reduction in the impurity concentration or moderate doping with one type of impurity would serve to suppress this effect.

As discussed in Section III, the solubility of most impurities in ice is in the ppm range or below and it is difficult to grow uniformly doped ice single crystals. It is possible on these accounts to explain the observed irreproducibility and lack of a more pronounced alteration of the overall vaporization rate in the doped samples. In fact, it is remarkable

that for dopants which were present in the ice in such small concentrations, there was any observable effect at all. Note that in Table I, the concentrations given are for the solutions from which the ice samples were grown, and note also that the only sample for which there was no reduction in the magnitude of rate fluctuation was the sample grown from a solution of trivalent $Cr(NO_3)_3$.

The results for ice doped with NH_4F must be discussed separately. As mentioned in Section III, the solubility of NH_4F in ice is appreciable, and it is likely (although no measurements were made) that the concentration of NH_4F in the ice samples whose rate is shown in Fig. 13 is less than a factor of 10 lower than the solution concentrations given. Also it should be remembered that HF is present in somewhat greater concentration in the lattice than in NH_3. Since HF (gas) has been observed to raise the vaporization rate and NH_3(gas) to lower it, it must be concluded that either NH_3 is considerably more effective than HF in altering the rate, or that their combined effect in the lattice as a salt is different than a simple summation of their effects separately as gases.

Finally it is important to note that for the impurities investigated there was no apprent tendency for them to build up on the surface and reduce the rate as vaporization progressed. This observation is corroborated by Fig. 17 which is an electron micrograph of an ice single crystal grown from a 0.01M solution of NH_4F and vaporized 1 min. at -100°C. The surface appears quite similar to the surface of a similar oriented pure ice single crystal after the same vaporization.

In the case of the 1M NH_4OH sample (Fig. 14) apparently NH_3 (which has a vapor pressure well above that of ice) vaporized until a congruently vaporizing mixture was obtained. It is worthwhile to point out that since

for this case a constant α_v was observed to very high rates, it is unlikely that the departure from unity for α_v observed for other samples is due to surface cooling. Had surface cooling been an important effect, the pronounced curvature that was exhibited in the rate plots for all other samples would have been seen for this sample as well.

3. Gas Effects

The retardation and increase in the ice vaporization rate in the presence of NH_3(gas) and HF(gas) respectively can give extra information about the vaporization mechanism and is discussed in Section VI.

VI. ICE VAPORIZATION MECHANISM

In preceding sections, principles of vaporization, structure and properties of ice, and the measured ice vaporization kinetics have been discussed. In this section, a model consistent with these facts is proposed to explain on a molecular scale the detailed steps by which molecules of the solid enter the vapor. The vaporization of pure ice is described first and then the influence of impurities is discussed.

The following statements summarize the experimental observations which may be of value in determining the vaporization mechanism of ice single crystals.

(1) The vacuum sublimation rate of pure ice has been measured in the temperature range of -90° to -40°C. The sublimation rates of the different samples were reproducible with ~ ± 10% and were not dependent on crystal orientation (basal face vs. prism face) or on crystallinity (single-crystal vs. polycrystalline samples). The steady-state sublimation rate is rapidly attained at a given temperature.

(2) The plot of log J_{obs} vs T^{-1} is a curve with a characteristic shape for all ice samples (except those grown from concentrated solutions of NH_4F and NH_4OH). The activation enthalpy of sublimation ΔH_s^* is equal to the equilibrium enthalpy of sublimation ΔH_s° at low temperatures (< - 85°) and approaches a limiting value of about 1/2 ΔH_s° at high temperatures (> - 40°).

(3) Ionic impurities in ice appear to cause a shift in the characteristic sublimation rate curve (decrease the sublimation rate). The impurities do not have a cumulative effect on the rate and do not appear to collect on the surface.

(4) NH_3(gas) impinging on the vaporizing surface causes a reduction in J_{obs}; HF (gas) impinging on the vaporizing surface causes an increase in J_{obs}.

(5) The vaporization of polymers (dimers, trimers, etc.) does not occur to any significant extent.

(6) The surface of freely vaporizing ice is smooth (apart from transient etch pits) in the temperature range for which $\alpha_v = 1$ ($< -85°$) and becomes increasingly rough in the temperature range ($> -85°C$) for which $\alpha_v < 1$.

(7) The sintering of ice is severely retarded in a dry atmosphere.

(8) Water molecules are hydrogen-bonded to at most 4 nearest neighbors. Using structural models and experimental information it is possible to distinguish between water water molecules which have, in turn, 4,3,2, and 1 hydrogen bondsto other water molecules.

The ball- and stick model of ice of Fig. 6 is small enough so that all but one of the "molecules" are part of a surface: of the 39 molecules represented there are eight molecules with 4 nearest neighbors (4 bonded), twenty-two with 3 nearest neighbors (3-bonded) and nine with 2 nearest neighbors (2-bonded). No molecules with only 1 nearest neighbor (1-bonded) are shown but they may be imagined as admolecules on one of the surfaces.

A smooth low-index ice surface contains equal numbers of 4-bonded and 3-bonded molecules; a ledge on the surface will necessarily have a large number of 2-bonded molecules. A rough surface is one with many ledges and it is not unreasonable that the number of 2-bonded molecules on a rough surface should be of the same magnitude as the number of 3-bonded and 4-bonded.*

---

*Roughening of the low-index faces of ice at equilibrium has been treated by Yosida (1967).

In order to arrive at a model of the ice vaporization mechanism which is consistent with the experimental evidence the following assumptions are made:

(1) The oxygen lattice extends to the surface without major rearrangement.

(2) The positions of the hydrogens do not need to be considered as they are randomly arranged.

(3) 2-bonded water molecules are present on the surface of freely vaporizing ice in a concentration W^2 that is of the same magnitude as the concentration of 3-bonded and 4-bonded water molecules W^3 and W^4, (due to surface roughness, i.e. large ledge concentration), and consequently does not change markedly with temperature.*

(4) 1-bonded molecules are uniformly distributed over the ice surface. These admolecules are most likely the high-surface-mobility species responsible for sintering.** They are presumably of a considerably higher energy than the 2-. 3- and 4- bonded moleclues. At the temperatures included in the present study, their concentration W^1 will be small compared to the total number of molecules on the surface $N \sim 10^{15} cm^2$.

---

*This assumption may not be justified for temperatures near -85°C i.e., the region in which $\alpha_v \lesssim 1$, but as will be shown the vaporization rate is not very dependent on W^2 in this temperature region. It is worth while to point out that vaporization is not expected to alter the population of 3-bonded and 2-bonded molecules because they are replenished at the same average rate at which they are used up. Consider for example a 4-bonded molecule attached to a 2-bonded molecule, or a 3-bonded to a 1-bonded. After breaking their mutual bonds, the resulting molecules are 3, 1, 2 and zero-bonded, respectively. Note that the superscript is used here merely to distinguish the various species.

**Murphy (1953) has proposed that these molecules might owe their mobility to a kind of "bipedal random walk" in which a molecule is alternately 1-bonded and 2-bonded as it moves across the ice surface.

The proposed vaporization mechanism is

$$W^2 \underset{k_{12}}{\overset{k_{21}}{\rightleftharpoons}} W^1 \underset{k_{01}}{\overset{k_{10}}{\rightleftharpoons}} W^0$$

where W^2 and W^1 are the concentrations of 2-bonded and 1-bonded water moleclues respectively on the ice surface and W^0 is the concentration of water vapor molecules. Note that W^i is used to refer both to an i-bonded molecule and to its concentration. The double-index notation on the rate constants k_{ij} is used to denote the passage from state i to state j.

The corresponding rate equations are

$$j_{21} = k_{21} W^2; \quad j_{12} = k_{12} W^1; \quad j_{10} = k_{10} W^1; \quad j_{01} = k_{01} W^0.$$

The rate "constants" may be expressed:

$$k_{21} = \nu_{21} \exp(\sigma_{21}/k) \exp(-\epsilon_{21}/kT)$$
$$k_{12} = \nu_{12} f W^2 \exp(\sigma_{12}/k)$$
$$k_{10} = \nu_{10} \exp(\sigma_{10}/k) \exp(-\epsilon_{10}/kT)$$
$$k_{01} = \alpha_c \exp(\sigma_{01}/k) O$$

The v_{ij} are generalized temperature-independent frequencies, the σ_{ij} are the appropriate entropy changes and the ϵ_{ij} are the energy differences between states i and j. The rate constant k_{12} depends on the availability of sites suitable for a 1-bonded molecule to become a 2-bonded molecule and this is taken to be linearly proportional (by a factor f) to the concentration W^2 of 2-bonded molecules. Note that for free vaporization $j_{01} = 0$ even though neither k_{01} nor $W^0 = 0$; this apparent paradox is resolved by recalling that j_{01} requires a velocity distribution in W^0 that includes that molecules incident on the surface; k_{01} is written to contain an operator O that selects the incident population from W^0.

At steady-state $dW^1/dt = j_{21} - j_{12}' - j_{10} = 0$;

$$k_{21} W^2 - k_{12} W^1 - k_{10} W^1 = 0; \quad W^1 = \frac{k_{21} W^2}{k_{12} + k_{10}} \tag{3}$$

Thus
$$j_{10} = J_{obs} = k_{10} W^1 = \frac{k_{10} k_{21} W^2}{k_{12} + k_{10}}$$

The two limiting case are:

Case I: $k_{10} \ll k_{12}$. Then $J_{obs} \simeq k_{10}(k_{12}/k_{12}) W^2$

$$J_{obs} = \nu_{10}(\nu_{21}/f\nu_{12}) \exp [(\sigma_{10} + \sigma_{21} - \sigma_{12})/k] \exp [- (\epsilon_{21} + \epsilon_{10})/kT]$$

Case II: $k_{10} \gg k_{12}$. Then $J_{obs} \simeq k_{21} W^2 = \nu_{21} W^2 \exp (\sigma_{21}/k) \exp (-\epsilon_{21}/kT)$.

The energies ϵ_{21} and ϵ_{10} represents breaking of the third and fourth hydrogen bonds between a water molecule and its neighbors. As mentioned in Section III, a variety of values for the energy of a hydrogen bond in ice have been proposed. If we arbitrarily assign equal values to ϵ_{21} and ϵ_{10}, then since sublimation of one mole of ice requires breaking two moles of bonds, we can say $\epsilon_{21} = \epsilon_{10} = 1/2\ \Delta H_s^\circ$.

Neglecting the difference between activation energy and the activation enthalpy ΔH_s^* discussed in Section II, the prediction of this model is that ΔH_s^* will be equal to ΔH_s° in Case I and $1/2\ \Delta H_s^\circ$ in Case II.

Considering now the experimental results it appears that Cases I and II describe ice vaporization below about -85°C and above about -40°C respectively, and that the complete expression given in Eq. 3 is required for the intermediate region.*

*An actual calculation using Eq. 3 would require more knowledge about the various parameters and the possible temperature dependence of W^2 near -85°C.

Case I is a virtual equilibrium of all species on the ice surface: vaporization does not occur rapidly enough to disturb their equilibrium populations. Case II is a virtual depletion of the 1-bonded molecules: they vaporize as rapidly as they form. This high-temperature picture of mobile-species depletion is corroborated by the previously mentioned severe retardation of ice sintering in dry atmospheres.

By inspection of the equations it can be seen that Case I vaporization rates are proportional to the W^1 population, and Case II vaporization rates are proportional to the W^2 population. The effect of NH_3(gas) and HF(gas) in lowering and raising the vaporization rates at both low and high temperatures can be rationalized as follows:

As pointed out in Section III, each NH_3 or HF incorporated into the ice lattice produces a D or L defect. If the same condition prevails at the ice surface, each NH_3 molecule adsorbed produces a D-defect and each HF, an L-defect. With this explanation it is necessary to further postulate that only L-defects have a direct influence on the rate, since it seems unlikely that D-defects should themselves decrease the vaporization rate. In a manner comparable to that described by Jones and Glen (discussed in Section III), the rate-reducing influence of NH_3 would be to decrease the surface L-defect concentration below the level for pure ice. Alternatively stated the effect of these gases can be viewed as being due to their differing number of protons - the excess of one in NH_3 and the deficit of one in HF as compared to H_2O could shift the equilibria between surface species towards higher and lower numbers of hydrogen bonds respectively. It is not possible at present to consider this question in more detail since the surface concentration of Bjerrum

defects is unknown and the specific nature of the chemical interactions of gaseous NH_3 and HF with the surface has not been investigated.

The role of impurities other than NH_3 and HF on the properties of ice has not been as extensively studied. Kelley and Salomon (1969) show that the dielectric relaxation time decreases and the activation energy increase with increasing concentrations of NaOH in the ice lattice. This observation is consistent with a general increase in lattice binding energy attributable to long-range ionic interactions. On the other hand NH_4F causes a large decrease in the dielectric relaxation activation energy. Causes for this effect have been propsed (Gross, 1968) but remain uncertain.

The shape of the vaporization curve for doped ice samples indicates that at low temperatures ΔH_s^* is still equal to ΔH_s°-- doping does not change the slope and equilibrium between W^2 and W^1 surface species is maintained but shifted towards W^2. Doping thus appears to cause a reduction in the equilibrium population of W^1 on the vaporizing ice surface and consequently a reduction in the vaporization rate at temperatures for which desorption of W^1 molecules is the rate - determining step. Because the doping levels attainable were low and non-uniform it is difficult to draw firm conclusions about the exact role of impurities. However, from the fact that they do not have a cumulative effect on the vaporization rate and do not pile up on the surface it is possible to rule out any permanent blocking of surface sites.

VII. CONCLUSIONS

It now appears that the behavior of the ice surface during vacuum sublimation can be understood, at least in part. (The development of the asperities at low temperatures and whiskers at high temperatures await explanation.) Ice at equilibrium with its vapor at a given temperature appears to have a population of mobile surface molecules, perhaps hydrogen-bonded to only one other water molecule at a time. At very low temperatures vacuum sublimation does not occur rapidly enough to disturb the population of mobile species from its equilibrium value and desorption of these molecules from the surface to become vapor is the rate-limiting step. Consequently, the vaporization rate can be calculated from the equilibrium vapor pressure. The activation enthalpy of sublimation ΔH_s^* is equal to the equilibrium enthalpy of sublimation ΔH_s° ($\Delta H_s^* = \Delta H_s^\circ = 12.2$ kcal mole^{-1}).

At temperatures above about -85°C, the vacuum sublimation rate is rapid enough that it begins to deplete the population of mobile surface molecules to a concentration below the equilibrium value and the observed rate begins to fall below the theoretical maximum rate. At about -60°C this departure becomes quite marked. The activation enthalpy appears to approach the lower limiting value of $\Delta H_s^* = 6\text{-}1$ kcal mole^{-1}. Other indications which point to the depletion of mobile molecules are surface roughening that develops above -85°C, and the failure of ice to sinter in a dry atmosphere (far from ice-vapor equilibrium). At temperatures above about -40°C, the vaporization rate is completely controlled by the rate of production of mobile surface molecules.

Ionic and Bjerrum defects are not expected to play an important role in the vaporization of pure ice. However, impurities in the ice lattice do influence the kinetics (they decrease the vaporization rate). It may be that they increase the binding energy of the water molecules in the ice lattice somewhat due to long-range coulombic interaction. The rate reduction is particularly prominent in ice grown from 1 M NH_4F -- more than an order of magnitude. The effects of impurities on the sublimation rate of ice cannot yet be assessed fully due to the lack of better information on their solubility in the ice lattice. In the presence of NH_3 (gas) (10^{-3} to 10^{-2} torr) the ice vaporization rate decreases while in the presence of gaseous HF the rate increases. It is proposed that NH_3 and HF are chemisorbed on the ice surface and produce D- and L- defects, respectively in excess of their equilibrium concentrations. The increased concentration of L-defects increases the vaporization rate. It appears that at sufficiently high gas pressures these gases alter the L defect concentration enough to measurably alter (by ~10%) the ice vaporization rate.

TABLE I

α_v at $T^{-1} = 4.8\ 10^{-3}\ °K^{-1}$ (-65°C) for single crystals grown from solution by the Jona-Scherrer Method.

Dopant	Solution Concentration 0.01M	0.1M
NH_4OH	.80, .60	.64
LiOH	.73	.71
NaOH	.86	.87
HF	.77, .73	
HNO_3		.78
NH_4F	.64	.40, .29
LiF	.73	.78
NaF	.80	.47, .54

APPENDIX: THE LITERATURE OF ICE

Information on ice is published in a variety of sources. I list below some major references that supply a collection of ice data.

1. N. E. Dorsey, Properties of Ordinary Water Substance, Reinhold Publishing Corp., 1940. Republished 1968 by Hafner. 673 pp., a compendium of all data on water in its various forms published through 1938.

2. D. Eisenberg and W. Kauzmann, The Structure and Properties of Water, Oxford University Press, 1969.

3. Bibliography on Snow, Ice and Permafrost with Abstract with a cumulative index for Vols. I-XVII. Contains over 20,000 abstracts of articles on ice. U.S. Army Cold Regions Research and Engineering Laboratory, Hanover, N.H.

4. D. Schulte--Frohlinde and K. Vacek, Radiation Chemistry of Aqueous Frozen Solutions, in Current Topics in Radiation Research, Vol. 5, pp. 39-74 (1969). Review and discussion with 94 references.

5. H. Oura, ed., Physics of Snow and Ice, International Conference on Low Temperature Science. I. Conference on Physics of Snow and Ice, Institute of Low Temperature Science, Hokkaido University. See especially Part 1, Section 1, Physical Properties of Ice, p. 1-479.

6. H. H. G. Jellinek, ed., J. Colloid and Interface Sci., 25, No. 2 Oct. 1967. A collection of 15 papers on the surface of ice presented at a symposium held at the 151st National Meeting of the American Chemical Society.

7. J. D. Bernal, ed., A Discussion on the Physics of Water and Ice, a collection of 12 papers published as Proc. Roy. Soc. A247, No. 1251, 21 October 1958.

8. B. J. Mason, ed., The Physics of Water and Ice, a collection of eight papers published as Advances in Physics (Quarterly Supplement to Phil. Magn) 7, No. 26, April 1958.

9. G. W. Gross, Some Effects of Trace Inorganics on the Ice/Water System, Chapter 3 in Trace Inorganics in Water, a symposium at the 153rd meeting of the American Chemical Society, published as a book, Advances in Chemistry Series, Vol. 73, 1968.

10. U.S. Army Cold Regions Research and Engineering Laboratory, a continuing series of Research Reports. See for example R. Brill and P. R. Camp, Properties of Ice, Research Report 68, May 1961. (Also available as AD277536).

11. N. Riehl, ed., Proceedings of the 3rd International Symposium on the Physics of Ice (held in September 1968) (Plenum Press, New York), published June 1969. An up-to-date collection of a large number of papers.

12. Some Physics Titles on Ice (1960-1964), compiled and kindly supplied by M. Kopp, 401 - 2X23 Westinghouse Electric Corporation Research and Development Center, Churchill Borough, Pittsburgh, Pa. 15235. 21 pages of references.

ACKNOWLEDGEMENTS

I am deeply indebted to my research advisor Gabor A. Somorjai under whose guidance this work has been carried out, and I am grateful to members of the research group for many helpful and stimulating discussions, particularly Whalun Szeto for his assistance in electronic equipment design. I had several valuable discussions with Professor Leo Brewer, and am happy to acknowledge the collaboration of Professor Daniel Branton on the electron microscopic studies. Thanks also are due to Richard Williams and Susan Whytock for technical assistance on some of the experiments, my wife Nancy for encouragement and understanding and to Professor and Mrs. Joel Hildebrand for providing housing during part of the time the thesis was in preparation. My research was performed under the auspices of the Atomic Energy Commission.

REFERENCES

Alty, T., 1937 Proc. Roy Soc. 161, 68.

Baranaev, M. K., 1946, Zhur. Phyz. Chim. 20, 399. (In Russian).

Barnaal, D. E., and I J. Lowe, 1968, J. Chem. Phys. 48, 4614.

Burrows, G., 1954, Trans. Instr. Chem. Engrs. 32, 23.

Burrows, G., 1957, J. Appl. Chem. 7, 375.

Cross, J. D., 1969, Science 164, 174.

Cross, J.D. and P. A. Speare, 1969, Brit. J. Appl. Phys. 2, 1021.

Davy, J. G., 1970, Vacuum Microbalance Apparatus for Rapid Determination of Low-Temperature Vaporization Rates, in Vacuum Microbalance Techniques (Plenum Press, New York) Vol. 8, to be published.

Davy, J. G. and D. Branton, 1970, paper on electron microscopy of vaporizing ice surface, submitted to Science.

Deamer, D. W. and D. Branton, 1967, Science, 158, 655.

Delaney, L. J. et. al., 1964, Chem. Eng. Sci. 19, 105.

de Micheli, S. M. and A. R. Licenblat, 1967, J. Atmospher. Sci. 24, 312.

Dorsey, N. E., 1940, Properties of Ordinary Water-Substance (Reinhold Publishing Corp., New York; republished by Hafner, New York, 1968 673 p), p. 600.

Dushman, S., 1962, Scientific Foundations of Vacuum Techniques (J. M. Lafferty, ed.) (John Wiley and Sons, Inc, New York) 2nd ed., p. 726.

Eisenberg, D. and W. Kauzmann, 1969. The Structure and Properties of Water (Oxford University Press), p. 47, 100.

Franck, E. U. and F. Meyer, 1959. Z. für Elektrochemic 63, 571. (In German).

Fukuda, A. and A. Higashi, 1969, Jap. J. Appl. Phys. 8, 993; abstract in Chem. Abstracts, 71: 85459v (1969).

Goff, J. A., 1942, Heating, Piping and Air Conditioning, p. 121, or Trans. Amer. Soc. Heat and Vent. Engrs 48, 209 (identical articles).

Goff, J. A., and S. Gratch, 1946, Trans. Amer. Soc. Heat and Vent. Engrs 52, 95.

Greene, F. T. et al., 1969 Midwest Research Institute Summary Technical Report, 27 June 1967- 31 July 1969.

Gross, G. W., 1968, Some Effects of Trace Inorganics on the Ice/Water System, in Trace Inorganics in Water (American Chemical Society Advances in Chemistry Series), Vol. 73, p. 27.

Hamilton, W. C. and J. A. Ibers, 1968, Hydrogen Bonding in Solids, (W. A. Benjamin, Inc., New York), p. 191.

Heinmets, F., 1960, Nature, 188, 925.

Hirth, J. P. and G. M. Pound, 1963, Condensation and Evaporation (Pergamon Press, Oxford), Progress in Materials Science, Vol. 11, p.9.

Isono, K. and K. Iwai, 1969, Nature 223, 1149.

Jaccard, C. and L. Levi, 1961, Z. Angewandte Math u. Physik 7, 70. (In French).

Jellinek, H. H. G., 1957. J. Colloid and Interface Sci. 25, 192.

Jona, F. and P. Scherrer, 1952, Helv. Phys. Acta, 25, 35. In German. For a discussion in English, see R. Siksna, 1957, Arkiv för Fysik 11, 495.

Jones, S. J. and J. W. Glen, 1969, Phil. Mag. 19, 13.

Kelley, D. J. and R. E. Salomon, 1969, J. Chem. Phys. 50, 75.

Kelley, K. K., 1935, Contributions to the Data on Theoretical Metallurgy, Vol. III (U.S. Bureau of Mines Bulletin 383), p.51.

Koros, R. M. et. al., 1966, Chem. Eng. Sci. 21, 941.

Kramers, H. and S. Stemerding, 1951, Appl. Sci. Res. A3, 73.

Kröger, F. A., 1964, The Chemistry of Imperfect Crystals, (North-Holland, Amsterdam), p. 750.

Labowitz, L. C. and E. F. Westrum, Jr., 1961, J. Phys. Chem. 65, 408.

List, R. J., 1951, Smithsonian Meteorological Tables (Smithsonian Institution, Washington, D. C.), Vol. 114, p. 350.

Lykov, A. V. et al., 1968, Inzh. Fiz. Zh. 15, 782. (In Russian).

Melville, H. W., 1936, Trans. Faraday Soc. 32, 1017.

Milne, T. A. and F. T. Greene, 1967, J. Chem. Phys. 47, 3668.

Murphy, E. J., 1953, J. Chem. Phys. 21, 1831.

Onsager, L. and L. K. Runnels, 1969, J. Chem. Phys. 50, 1089.

Pauling, L., 1935. J. Amer. Chem. Soc. 57, 2680.

Pimentel, G. C. and A. L. McClellan, 1960, The Hydrogen Bond, (W. H. Freeman and Co., San Francisco), p. 212.

Rosenblatt, G., 1963, J. Electrochem Soc. 110, 563.

Rossman, M. G. and J. Yarwood, 1954, Brit. J. Appl. Phys. 5, 7.

Somorjai, G. A. and J. E. Lester, 1967, Evaporation Mechanism of Solids in Progress in Solid State Chemistry (Pergamon Press, Oxford), Vol. 4, p.1.

Steinemann, A. and H. Gränicher, 1957, Helv. Phys. Acta 30, 553. (In German.)

Strickland-Constable, R. F. and E. W. Bruce, 1954, Trans. Instr. Chem. Engrs. 32, 192.

Tschudin, K., 1946, Helv. Phys. Acta, 19, 91 (In German).

Van Hook, W. A., 1968, J. Phys. Chem. 72, 1234.

Washburn, E. W., 1924, Monthly Weather Review 52, 488.

Webb, W. W. and C. E. Hayes, 1967, Phil. Mag. 16, 909.

Weber, S., 1915, Comm. Phys. Lab., Kammerlingh Onnes Laboratory, Leyden, No. 150a.

Whipple, F. J. W., 1927, Monthly Weather Review 55, 131.

Wood, 1964, Crystals and Light (D. Van Nostrand Co., Inc., Princeton, N.Y.), p. 94.

Wörz, O. and R. H. Cole, 1969, J. Chem. Phys. 51, 1546.

Yosida, Z., 1967, Surface Structure of Ice Crystal and Its Equilibrium Form, in Physics of Snow and Ice, International Conference on Low Temperature Science (Institute of Low Temperature Science, Hokkaido University) p. 1.

Young, J. G. and R. E. Salomon, 1968, J. Chem. Phys. 48, 1635.

FIGURE CAPTIONS

1. Schematic representation of a surface in the presence of its vapor.
2. Radiation-vaporization analog.
3. Semilog plot of equilibrium and kinetic data.
4. Vaporization rate measurements by various workers.
5. Electron micrograph of a prism face of an ice single crystal, vaporized one minute at -100°C. Square etch pits are characteristic of this face; direction of c-axis is indicated.
6. Ice I crystallizes in the wurtzite (ZnS) structure. Oxygen atoms are represented by balls (nearest-neighbor distance 2.76Å); hydrogen atoms (not shown) lie between oxygen (on the sticks), 0.99Å from one oxygen and 1.77Å from the other.
7. Representation of various low-index faces of ice: top view of basal or c-face and side views of five prisim faces -- two $\{11\bar{2}0\}$ faces and three $\{1\bar{1}00\}$ faces. Open curves are 0.9Å above closed circles. Directions of some prism axes are shown; c-axis is perpendicular to paper.
8. Preparation of oriented ice single crystals.
9. Low temperature vaporization system block diagram.
10. Microbalance vacuum chamber for low temperature vaporization.
11. Heat flow model.
12. Vaporization rates of undoped and high-purity ice.
13. Vaporization rates of ice grown from various solutions of NH_4F.
14. Vaporization rates of a sample quick frozen from 1M NH_4OH.
15. Effect of gas pressure and sample temperature on the vaporization rate of pure ice.

16a. Mean free path of water molecule in saturated water vapor as a function of temperature and saturated vapor pressure.

16b. Predicted worst-case behavior of ice vaporization rate for $\alpha_v = 1$ with decrease in mean free path.

17. Electron micrograph of the basal face of an ice single crystal grown from 0.01 M NH_4F solution and vaporized one minute at -100°C. Round etch pits are characteristic of this face.

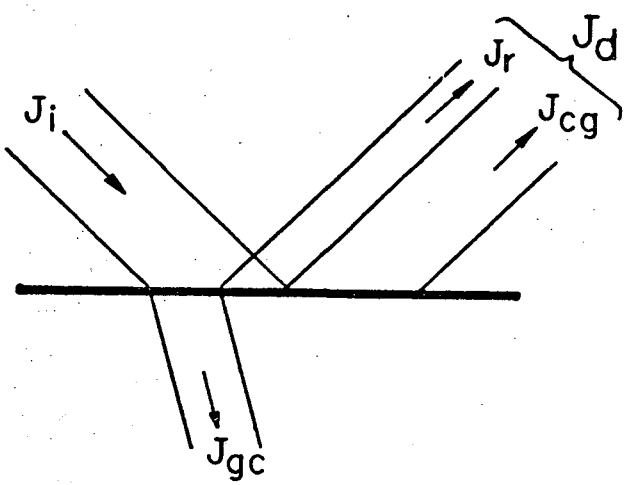

$$J_i = \frac{P}{\sqrt{2\pi mkT}}$$

$$\alpha_c \equiv \frac{J_{gc}}{J_i}$$

$$\alpha_v \equiv \frac{J_{cg}}{J_d^o} = \frac{J_{cg}}{J_i^o}$$

XBL694-2454

Figure 1

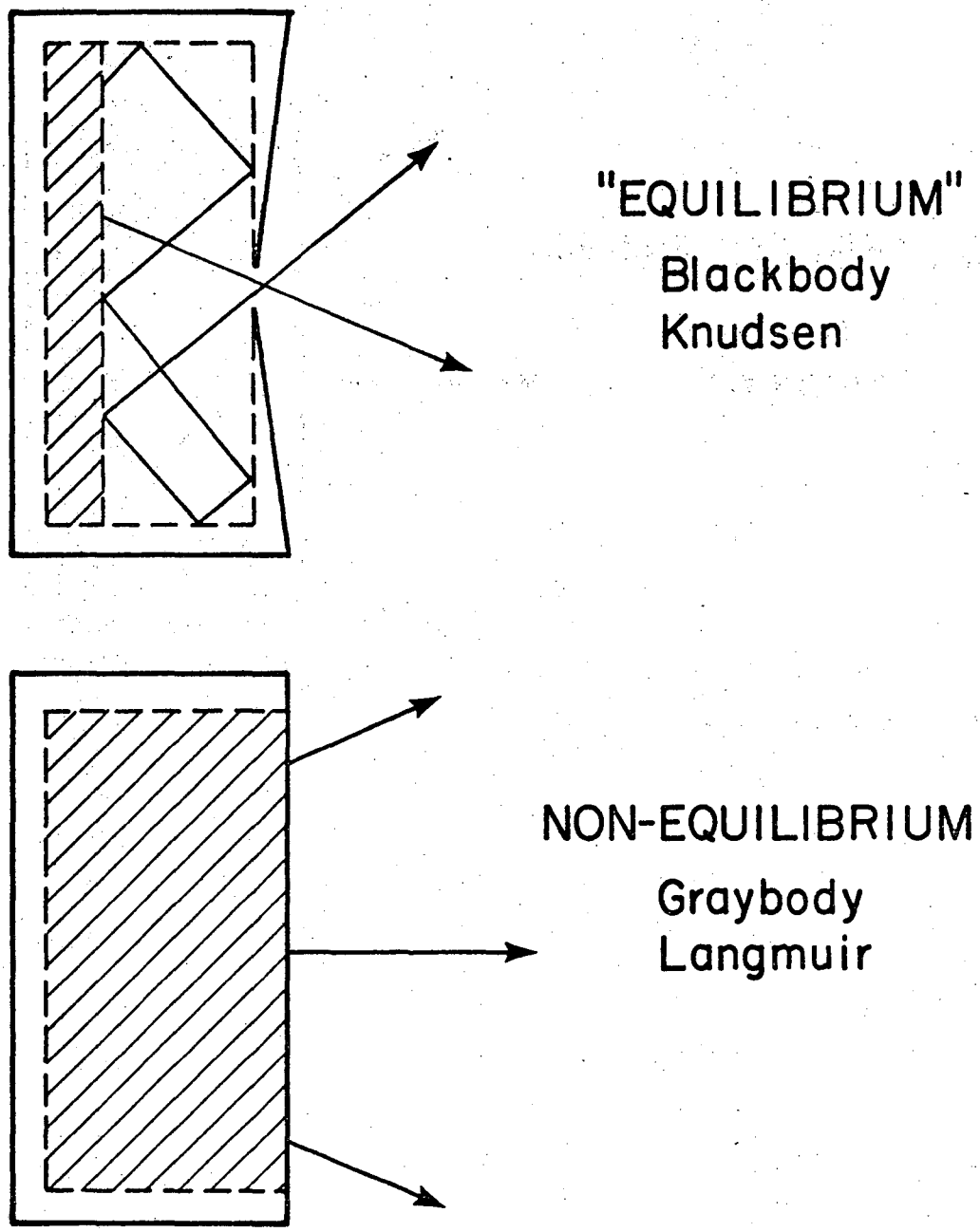

XBL 6912-6684

Figure 2

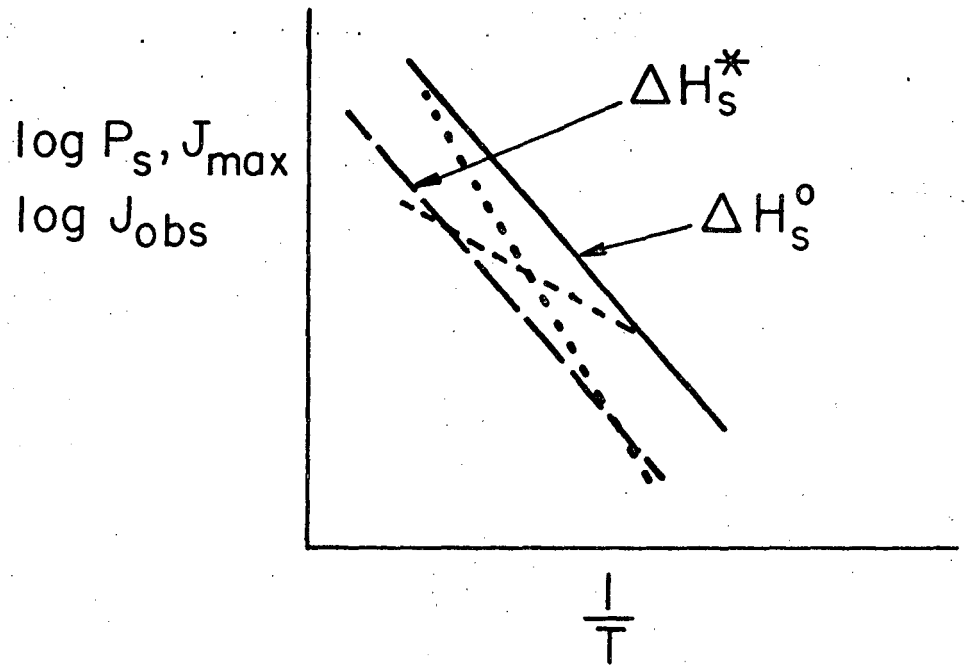

XBL694-2455

Figure 3

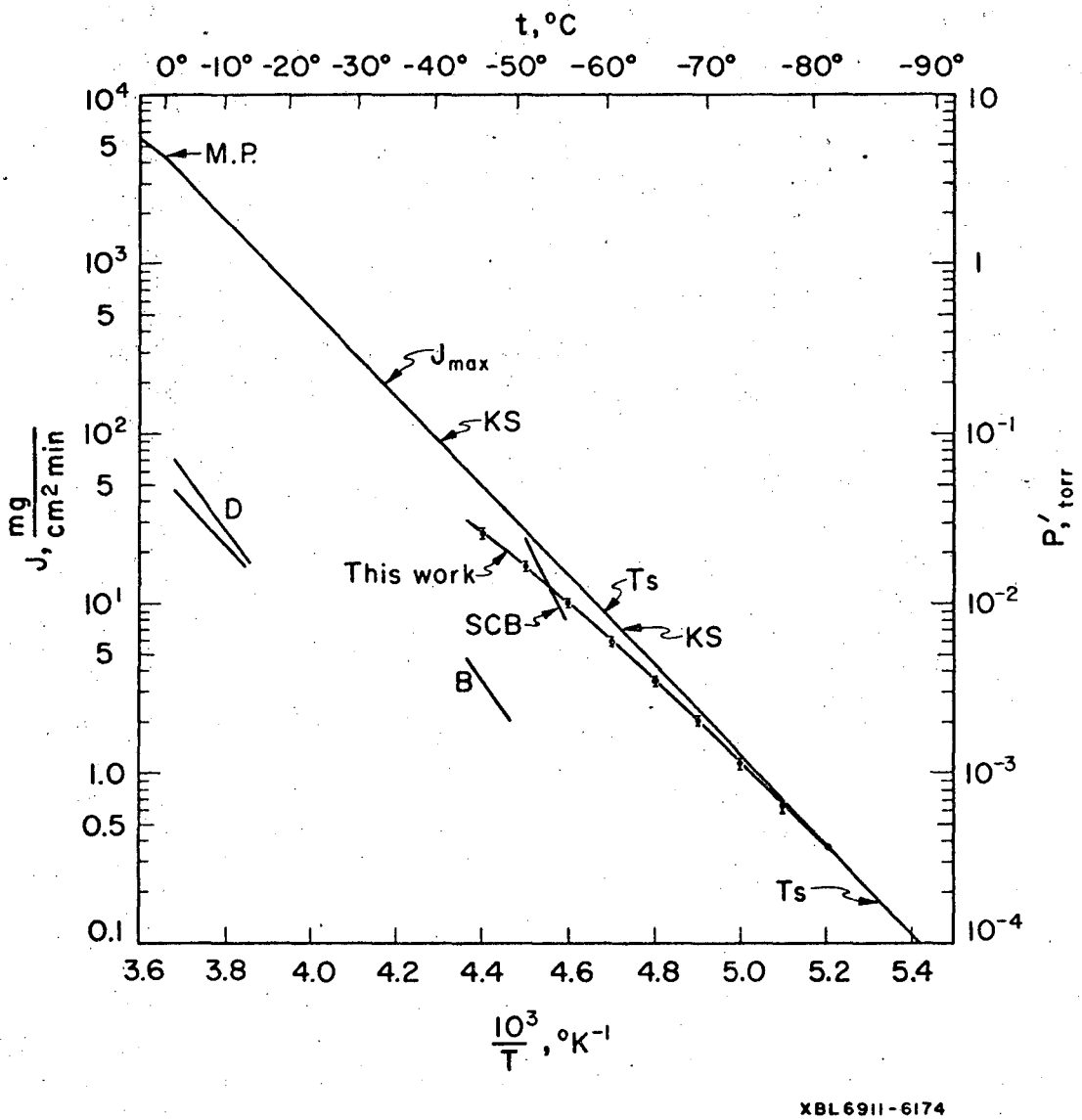
t, °C
0° -10° -20° -30° -40° -50° -60° -70° -80° -90°
M.P.
J_{max}
KS
D
This work
Ts
SCB
KS
B
Ts
$J, \frac{mg}{cm^2 min}$
$P', torr$
$\frac{10^3}{T}, °K^{-1}$
XBL6911-6174

Figure 4

XBB701-32

Figure 5

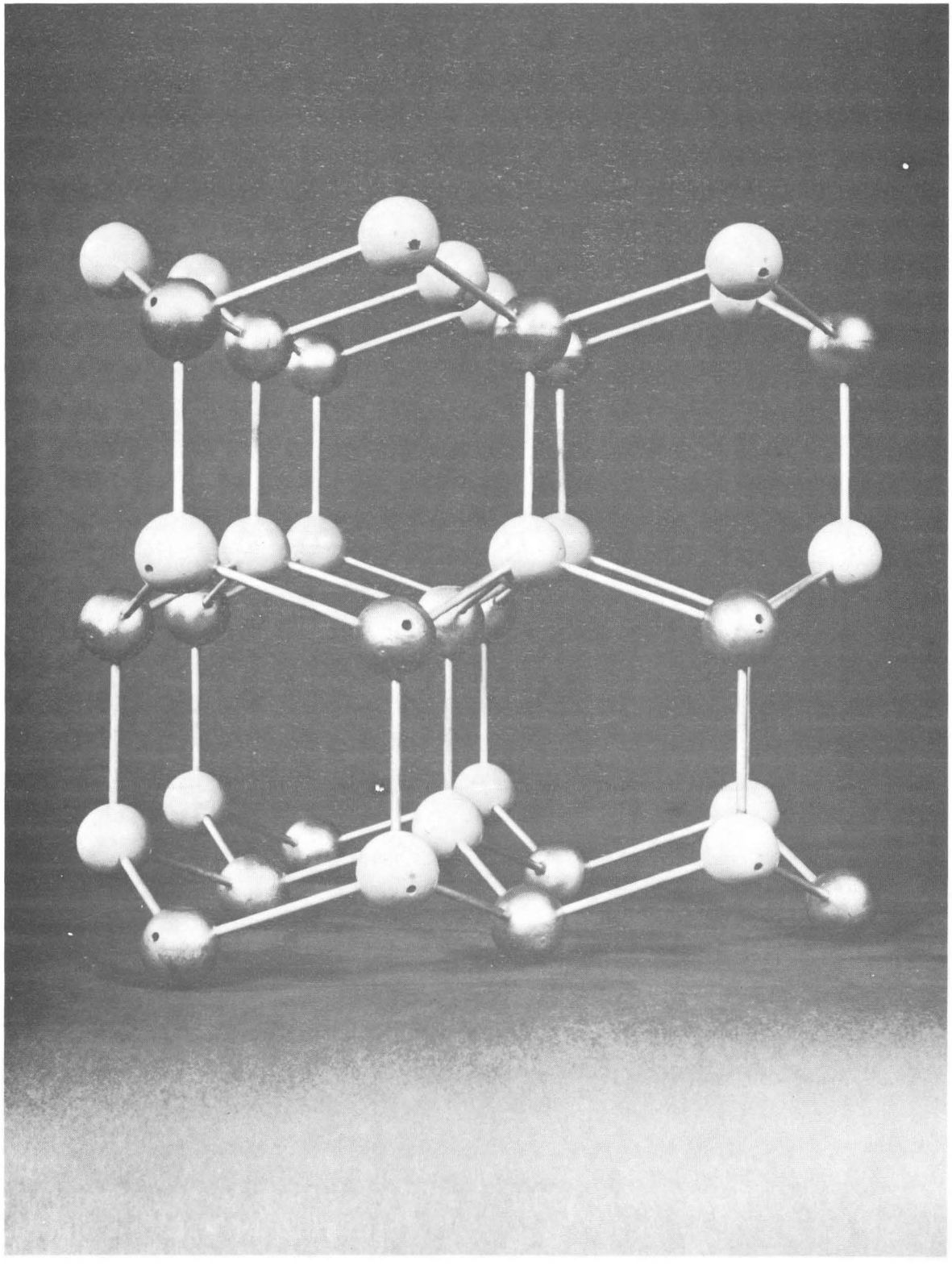

XBB692-1286

Figure 6

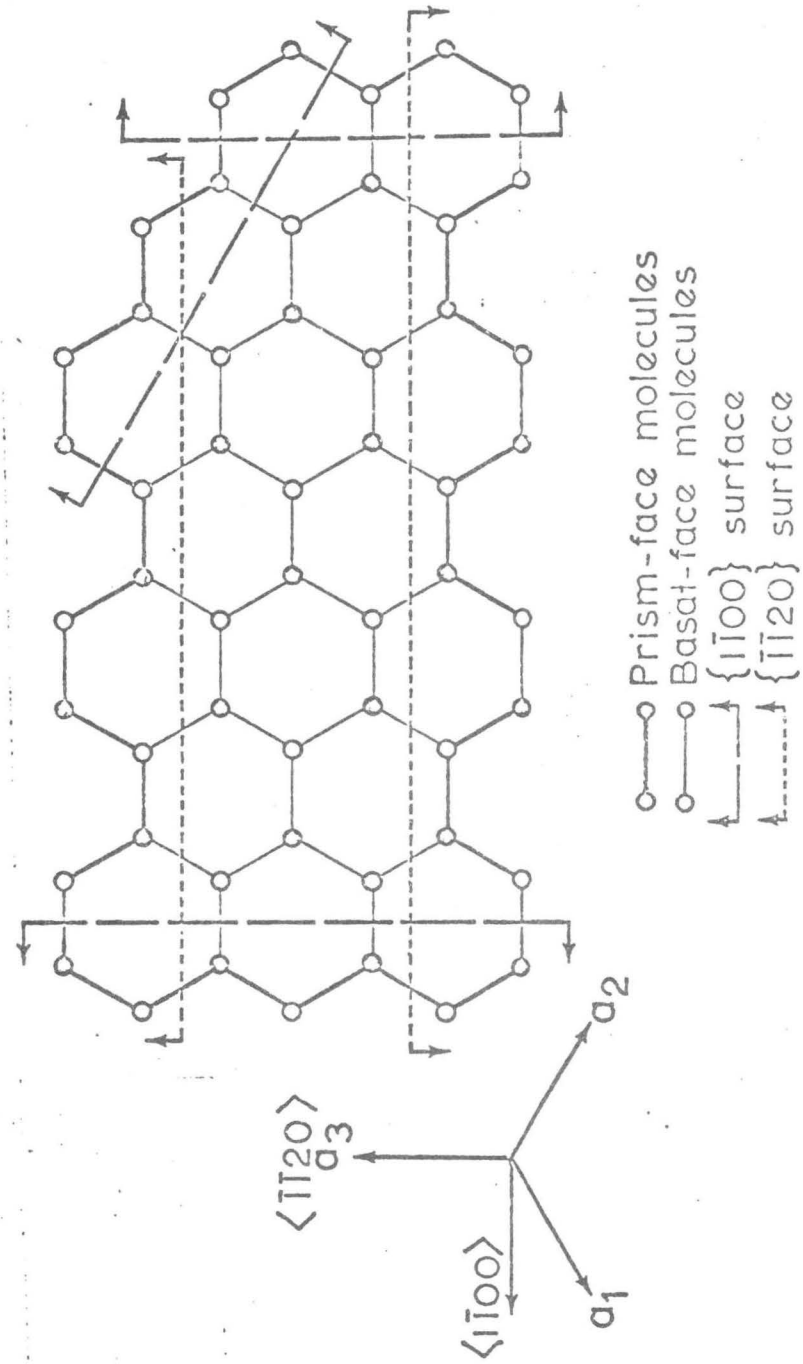
Prism-face molecules
Basal-face molecules
{1$\bar{1}$00} surface
{$\bar{1}\bar{1}$20} surface
a_2
a_1
a_3
⟨1$\bar{1}$00⟩
⟨$\bar{1}\bar{1}$20⟩

Figure 7

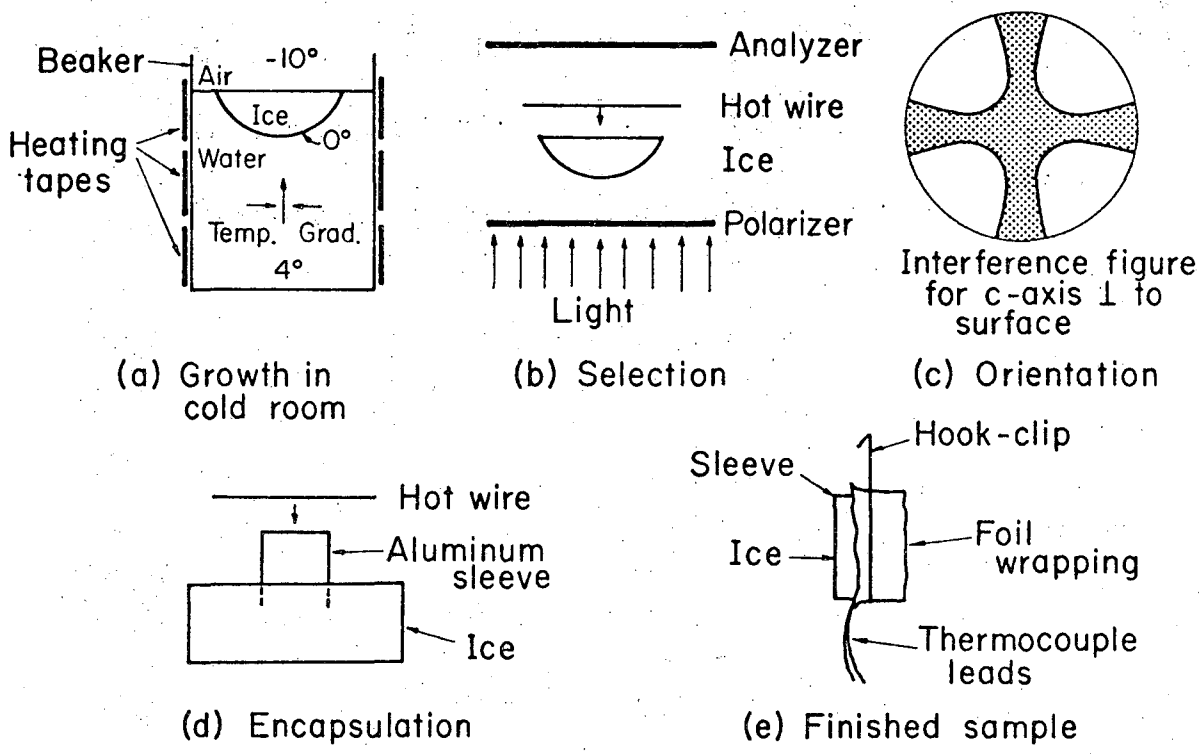

Preparation of oriented ice single crystals

XBL694-2488

Figure 8

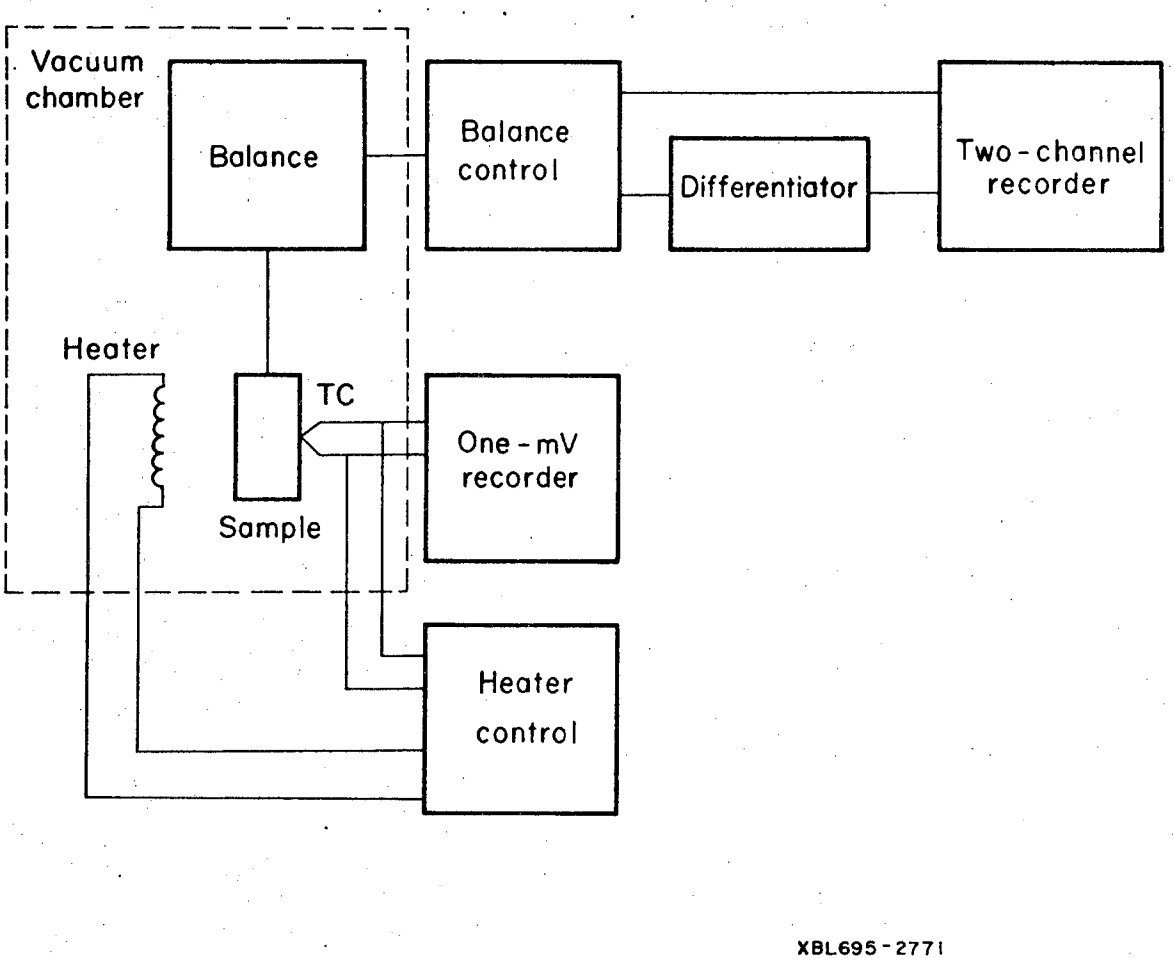
Vacuum chamber
Balance
Balance control
Differentiator
Two-channel recorder
Heater
TC
Sample
One-mV recorder
Heater control
XBL695-2771

Figure 9

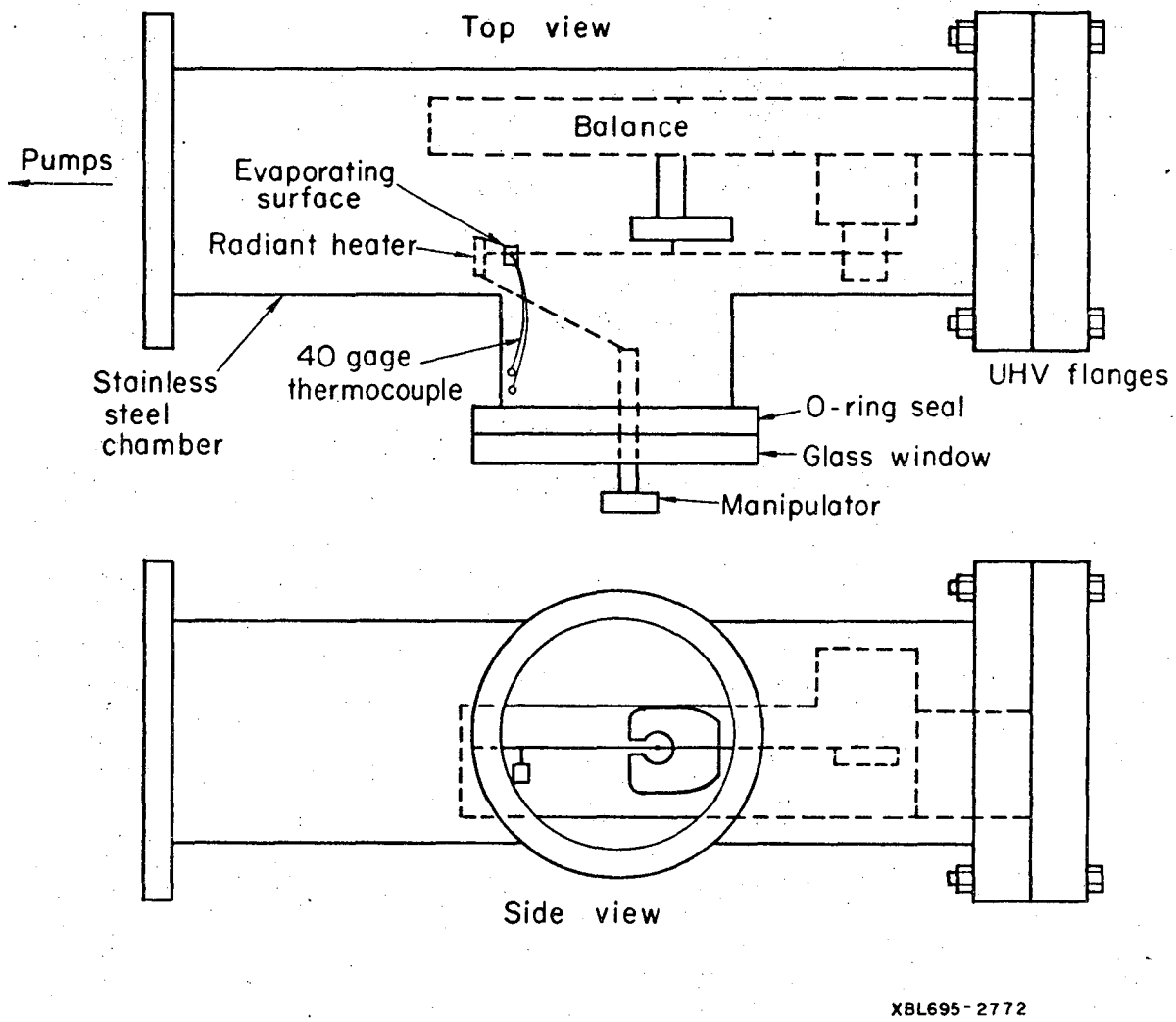
Top view
Balance
Pumps
Evaporating surface
Radiant heater
40 gage thermocouple
Stainless steel chamber
UHV flanges
O-ring seal
Glass window
Manipulator
Side view
XBL695-2772

Figure 10

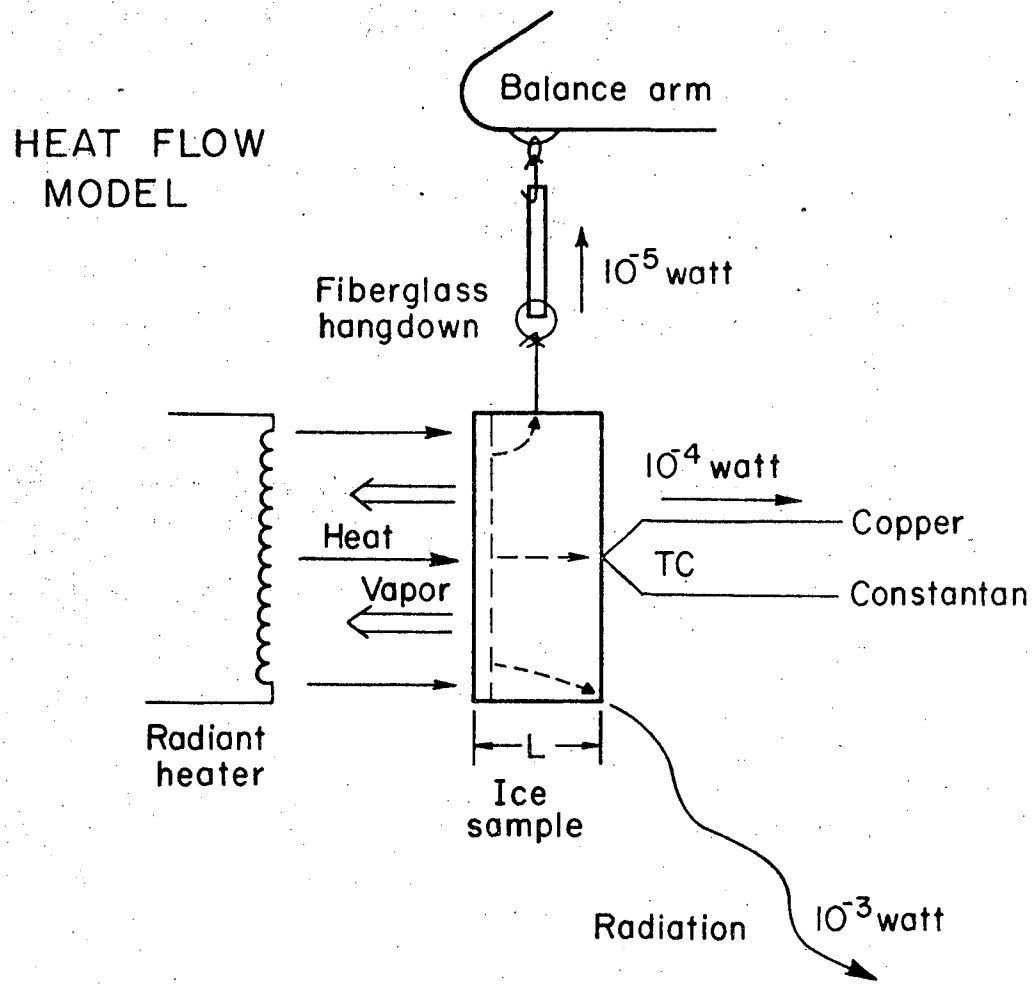

Steady-state solid-state thermal conduction

$$\frac{dT}{dx} = \frac{Q}{KA}; \Delta T = L\frac{dT}{dx} = 0.1\ °C$$

Sublimation power

t, °C	Q, mwatts
-70	43
-60	170
-50	660
-40	2000

XBL695 - 2773

Figure 11

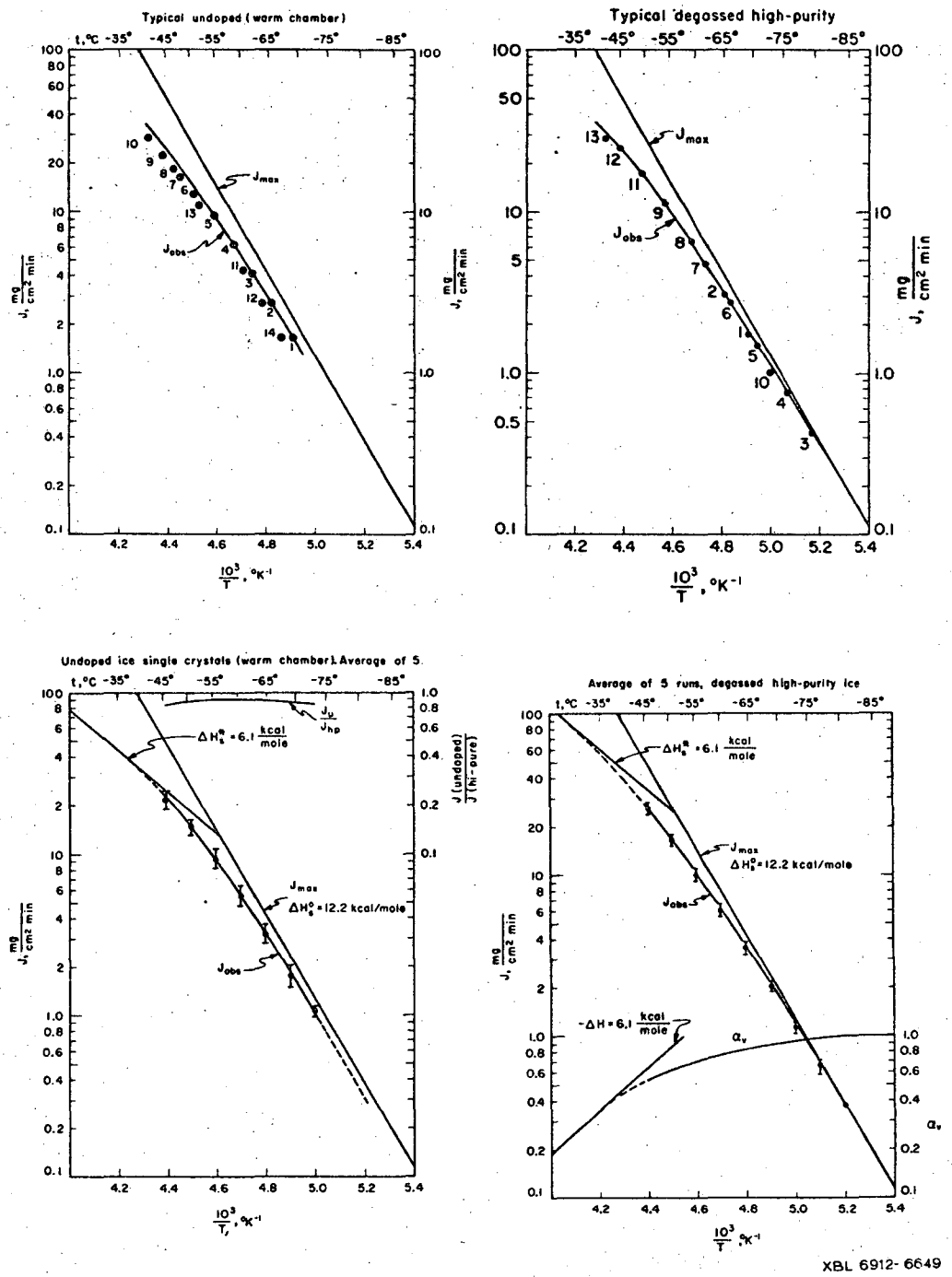
Typical undoped (warm chamber)
Typical degassed high-purity
Undoped ice single crystals (warm chamber). Average of 5.
Average of 5 runs, degassed high-purity ice
t, °C -35° -45° -55° -65° -75° -85°
J, mg/cm² min
10³/T, °K⁻¹
J_max
J_obs
ΔH_s° = 6.1 kcal/mole
ΔH_s° = 12.2 kcal/mole
-ΔH = 6.1 kcal/mole
α_v
J_u/J_hp
J (undoped)/J (hi-pure)
XBL 6912-6649

Figure 12

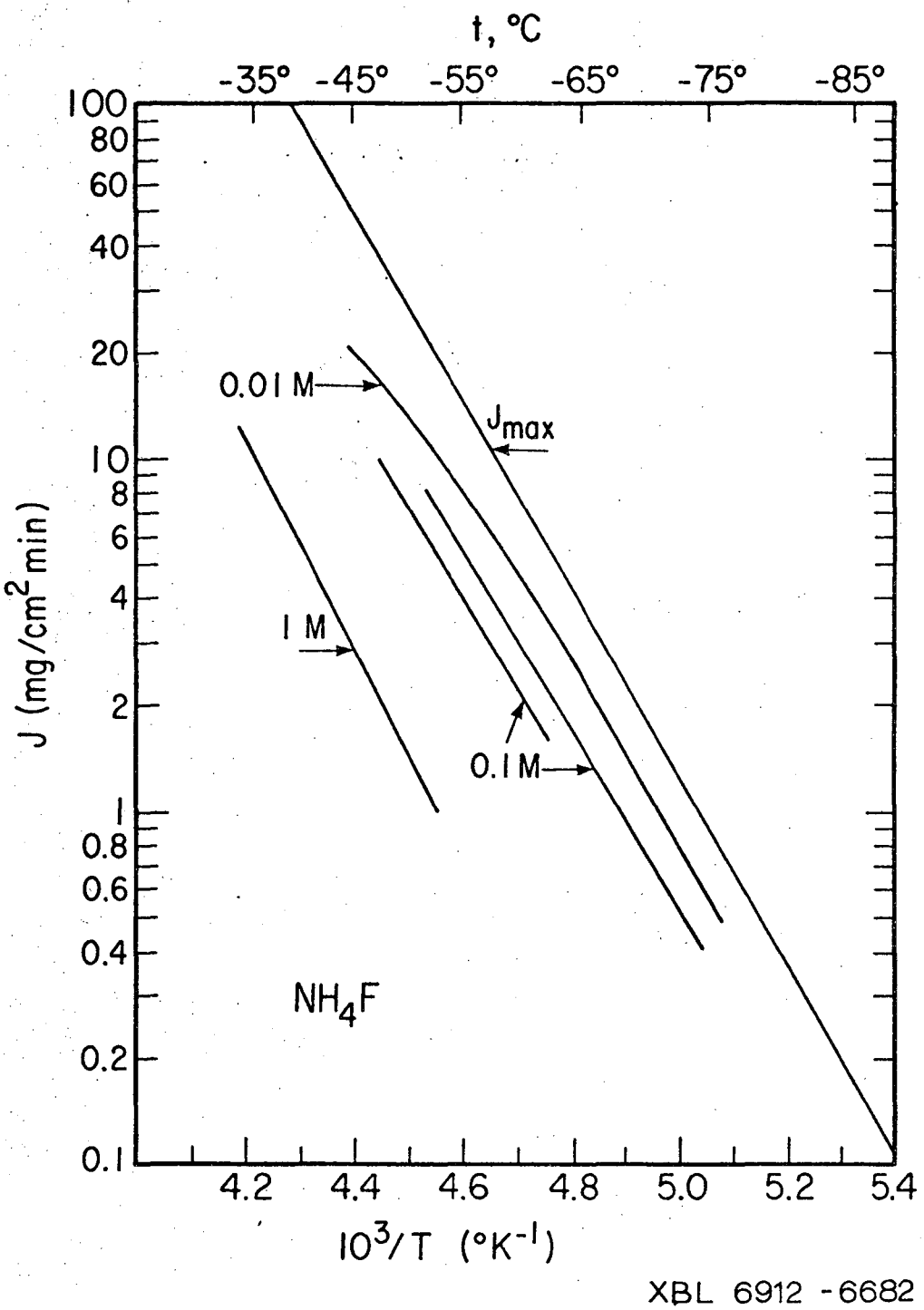
t, °C
-35°
-45°
-55°
-65°
-75°
-85°
100
80
60
40
20
10
8
6
4
2
1
0.8
0.6
0.4
0.2
0.1
J (mg/cm² min)
0.01 M
J max
1 M
0.1 M
NH4F
4.2
4.4
4.6
4.8
5.0
5.2
5.4
10³/T (°K⁻¹)
XBL 6912 -6682

Figure 13

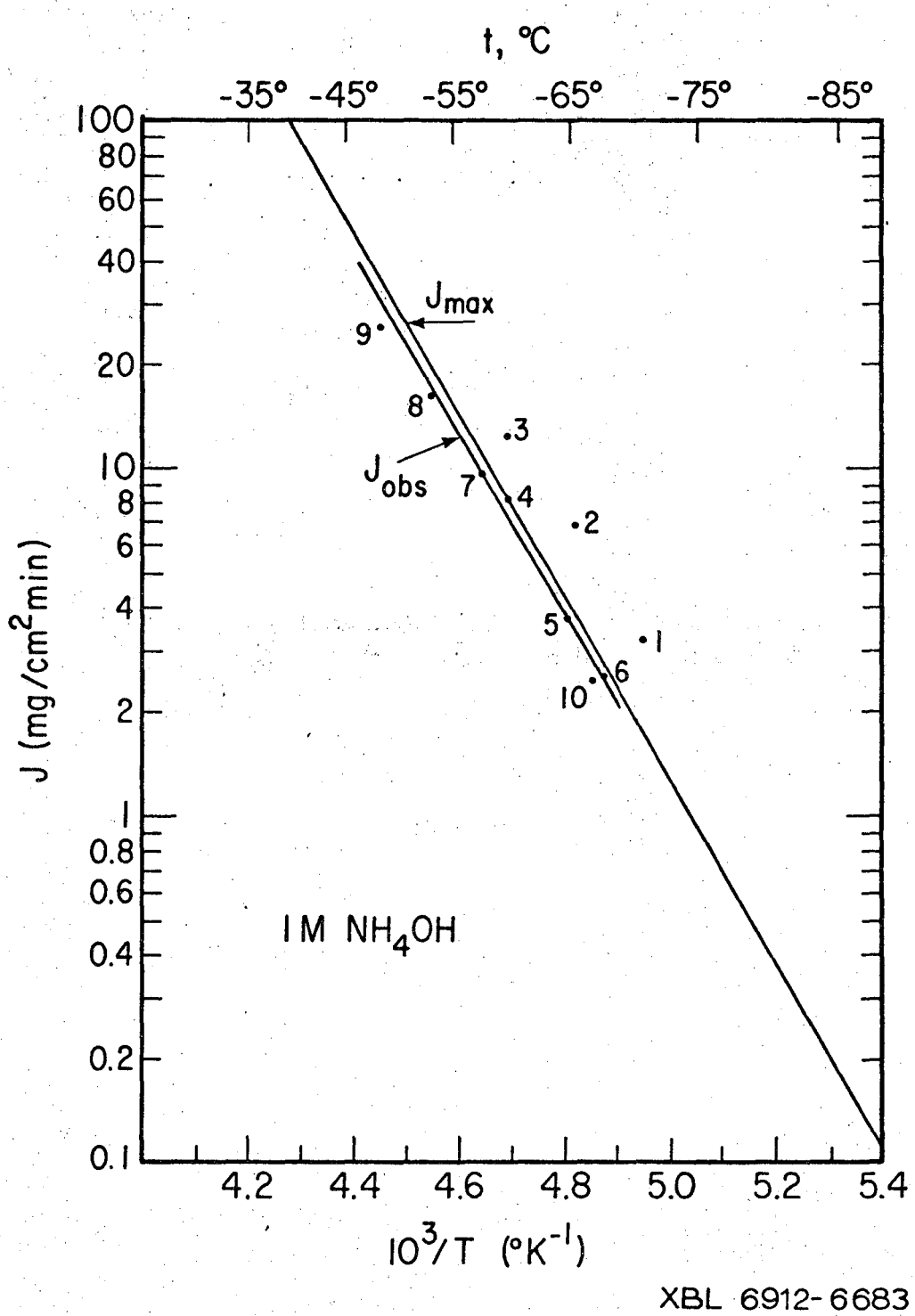
t, °C
-35° -45° -55° -65° -75° -85°
100
80
60
40
20
10
8
6
4
2
1
0.8
0.6
0.4
0.2
0.1
J (mg/cm²min)
Jmax
Jobs
9
8
3
7
4
2
5
1
6
10
1M NH4OH
4.2 4.4 4.6 4.8 5.0 5.2 5.4
10³/T (°K⁻¹)
XBL 6912-6683

Figure 14

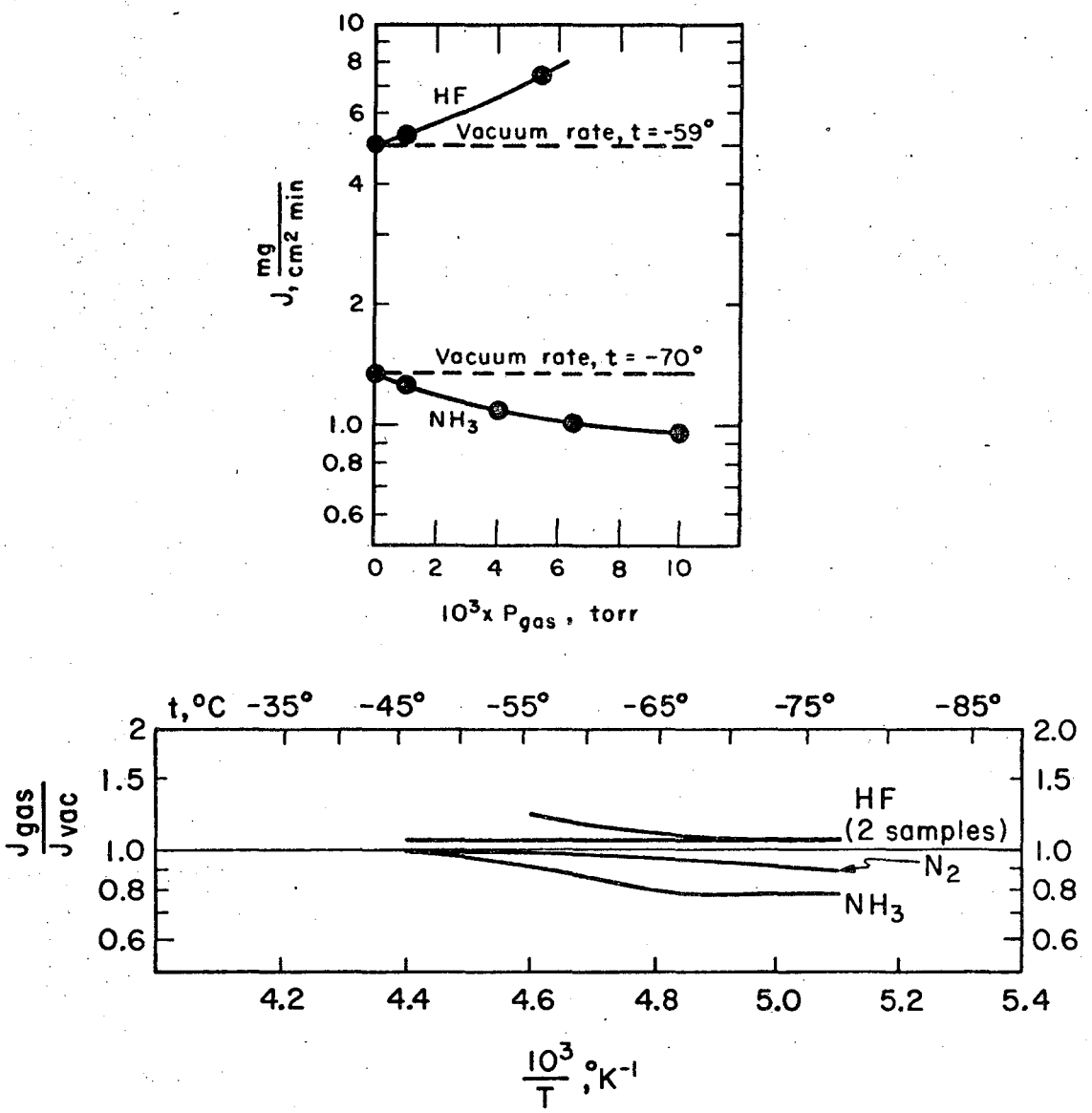

XBL 6912 -6663

Figure 15

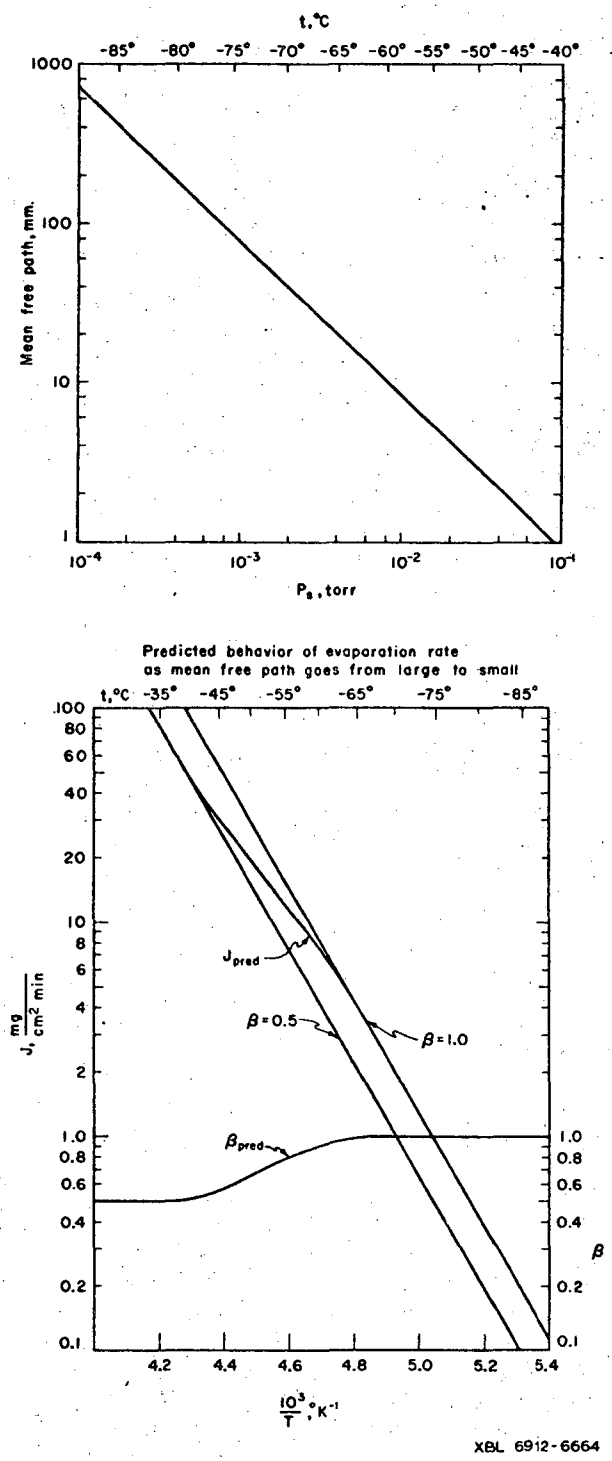
t, °C
-85° -80° -75° -70° -65° -60° -55° -50° -45° -40°
1000
100
10
1
Mean free path, mm.
10^{-4}
10^{-3}
10^{-2}
10^{-1}
P_s, torr
Predicted behavior of evaporation rate
as mean free path goes from large to small
t, °C -35° -45° -55° -65° -75° -85°
100
80
60
40
20
10
8
6
4
2
1.0
0.8
0.6
0.4
0.2
0.1
$J, \frac{mg}{cm^2\ min}$
J_{pred}
$\beta = 0.5$
$\beta = 1.0$
β_{pred}
β
4.2 4.4 4.6 4.8 5.0 5.2 5.4
$\frac{10^3}{T}$, °K^{-1}
XBL 6912-6664

Figure 16

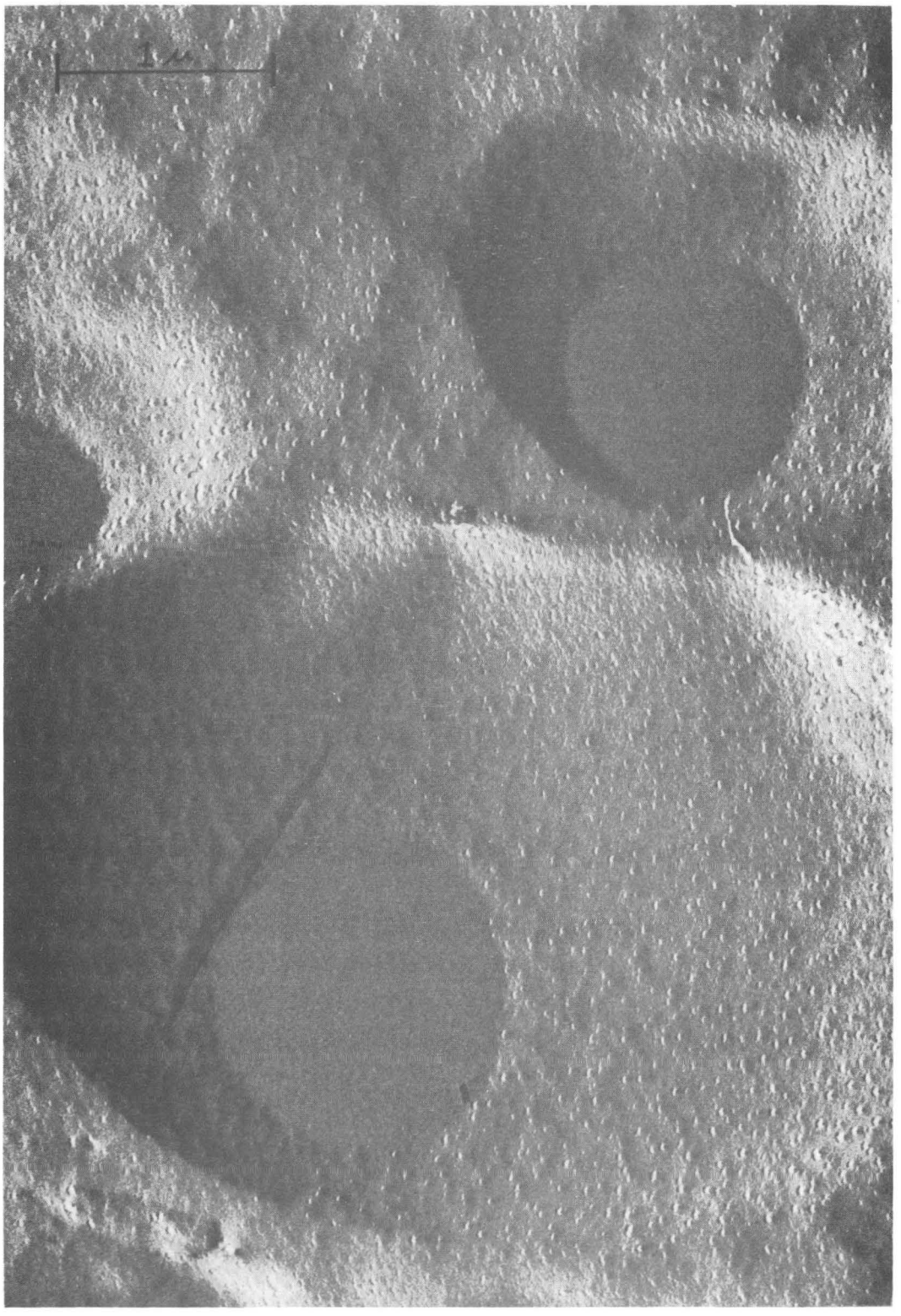

XBB701-31

Figure 17

LEGAL NOTICE

This report was prepared as an account of Government sponsored work. Neither the United States, nor the Commission, nor any person acting on behalf of the Commission:

A. Makes any warranty or representation, expressed or implied, with respect to the accuracy, completeness, or usefulness of the information contained in this report, or that the use of any information, apparatus, method, or process disclosed in this report may not infringe privately owned rights; or

B. Assumes any liabilities with respect to the use of, or for damages resulting from the use of any information, apparatus, method, or process disclosed in this report.

As used in the above, "person acting on behalf of the Commission" includes any employee or contractor of the Commission, or employee of such contractor, to the extent that such employee or contractor of the Commission, or employee of such contractor prepares, disseminates, or provides access to, any information pursuant to his employment or contract with the Commission, or his employment with such contractor.

TECHNICAL INFORMATION DIVISION
LAWRENCE RADIATION LABORATORY
UNIVERSITY OF CALIFORNIA
BERKELEY, CALIFORNIA 94720